

Formation and Evolution of Coherent Structures in 3D Strongly Turbulent Magnetized Plasmas

Loukas Vlahos^{a)} and Heinz Isliker^{b)}

Department of Physics, Aristotle University, 54124 Thessaloniki, Greece

(Dated: March 28, 2023)

We review the current literature on the formation of Coherent Structures (**CoSs**) in strongly turbulent 3D magnetized plasmas. CoSs (Current Sheets (**CS**), magnetic filaments, large amplitude magnetic disturbances, vortices, and shocklets) appear intermittently inside a turbulent plasma and are collectively the locus of magnetic energy transfer (dissipation) into particle kinetic energy, leading to heating and/or acceleration of the latter. CoSs and especially CSs are also evolving and fragmenting, becoming locally the source of new clusters of CoSs. Strong turbulence can be generated by the nonlinear coupling of large amplitude unstable plasma modes, by the explosive reorganization of large scale magnetic fields, or by the fragmentation of CoSs. A small fraction of CSs inside a strongly turbulent plasma will end up reconnecting. Magnetic Reconnection (**MR**) is one of the potential forms of energy dissipation of a turbulent plasma. Analysing the evolution of CSs and MR in isolation from the surrounding CoSs and plasma flows may be convenient for 2D numerical studies, but it is far from a realistic modeling of 3D astrophysical, space and laboratory environments, where strong turbulence can be exited, as e.g. in the solar wind, the solar atmosphere, solar flares and Coronal Mass Ejections (CMEs), large scale space and astrophysical shocks, the magnetosheath, the magnetotail, astrophysical jets, Edge Localized Modes (ELMs) in confined laboratory plasmas (TOKAMAKS), etc.

Keywords: Suggested keywords

I. INTRODUCTION

Strong turbulence is a complex nonlinear dynamic phenomenon, which has a great impact on the heating and acceleration of particles in space and laboratory plasmas^{1,2}. Unfortunately, courses for the study of turbulence are little present in university graduate programs. As a result, strong turbulence is also absent from the modeling of laboratory, astrophysical and space phenomena when they enter into a fully developed turbulent stage. The basic plasma physics courses at the universities start with the exploration of normal modes and linear instabilities. The nonlinear evolution of unstable waves is analysed with the use of the quasilinear approximation. In laboratory, space and astrophysical plasmas the "linear" phase of a normal mode has no meaning since the fluctuations grow in the presence of strong turbulence. The estimate of the growth time of the fluctuations in the presence of fully developed turbulence remains an open problem. Recently, Prof. William H. Matthaeus wrote a review article with the provocative title "*Turbulence of space plasmas: Who needs it?*"³ to stress the following fact: the scientific community avoids the use of strong turbulence in the interpretation of many astrophysical or laboratory plasma phenomena. Most studies treat the linear part of the evolution of a system very carefully, but when their models enter into the regime of fully developed turbulence, the intermittent appearance of Coherent Structures (CoSs) and their multi-scale evo-

lution fall beyond the ability of their numerical tools to handle them with present day computers. Therefore, the interpretations of many 3D strongly turbulent space and laboratory phenomena remain unexplored.

1. Weak vs strong turbulence

The study of turbulence can be divided into "weak" or "wave" turbulence and "strong" turbulence. We define as "weak" or "wave" turbulence the magnetic fluctuations resulting from the superposition of any spectrum of N linear modes,

$$\mathbf{b}(\mathbf{r}, t) = \sum_{i=1}^N \mathbf{b}_{0i} e^{i(\mathbf{k}_i \cdot \mathbf{r} - \omega(\mathbf{k}_i)t + \phi_i)}, \quad (1)$$

where \mathbf{k}_i is the wave vector, $\omega(\mathbf{k}_i)$ the dispersion relation derived through linearization, \mathbf{b}_{0i} the amplitude and ϕ_i the random phase of the the weakly damped/amplified wave mode i . This is a correct representation of a physical system if its unstable fluctuations have very small amplitude (i.e. for magnetized plasmas the fluctuations of the magnetic field \mathbf{b} are very weak, $|\mathbf{b}| \ll |\mathbf{B}_0|$, where \mathbf{B}_0 is the ambient magnetic field of the plasma).

In weak (wave) turbulence there is spectral transfer of energy through the resonant three wave interaction, analyzed with the use of the quasi linear theory and the prescribed energy dissipation at the small wave lengths^{4,5}.

Many references to "turbulence" in the current literature refer to "weak" turbulence, since its mathematical description is relatively easy, and with the use of the quasilinear approximation one can estimate the transport properties of the particles⁴. The regime where the

^{a)}<https://orcid.org/0000-0002-8700-4172>, vlahos@astro.auth.gr, corresponding author

^{b)}<https://orcid.org/0000-0001-9782-2294>, isliker@astro.auth.gr

unstable waves reach large amplitudes ($|\mathbf{b}| \geq |\mathbf{B}_0|$) is called “strong” turbulence if the turbulence is nearly isotropic^{6,7}. The non-linear evolution of the magnetic disturbances controls the energy transfer between the different scales and the particles. The most important characteristic of strong turbulence, which is not present in weak turbulence, is the intermittent appearance of CoSs. In this review, we focus on the 3D aspects of strong turbulence, and especially we address the question how CoSs are formed and evolve. The role CoSs play in the fast heating and acceleration of particles during explosive phenomena in astrophysical and laboratory plasmas is currently an open problem and cannot be addressed properly before having a good understanding of the statistical properties of the multi-scale evolution of CoSs⁸.

2. Intermittency and coherent structures

The magnetic energy and its dissipation in strongly turbulent systems is concentrated into intermittently appearing and disappearing CoSs. However, it is not well understood how CoSs are formed and distributed inside a turbulent volume. Also, the CoSs play a crucial role in how the dissipated energy is partitioned, and they operate on different scales⁹. An important assumption in fluid turbulence is that the energy injected at large scales is transferred to smaller and smaller scales by non-linear processes, where it is dissipated when it reaches the kinetic scales¹⁰. This process is known as the turbulent **energy cascade**. If CoSs of all sizes are distributed inside a strongly turbulent volume, the dissipation of energy via heating and acceleration of particles is distributed over all scales, and not only the small (kinetic) scales. 3D numerical simulations generally show turbulence to be quite intermittent, and scaling models have been developed to incorporate this effect¹¹. Particles interacting with a collection of CoSs (CSs, shocks, large amplitude magnetic perturbations) on all scales gain or lose energy as they travel through the turbulent volume before escaping¹². It is not apparent how the energy is dissipated on the different scales, and a detailed study is needed to clarify this point.

As we are going to show in this review, turbulence can generate, among other types of CoSs, current sheets (CSs) at all scales, and it has been proposed that a fraction of the CSs undergo magnetic reconnection as part of their dissipation process¹³. It is important to stress that CSs are only one of the many types of CoSs appearing in strongly turbulent magnetised plasma. The other types include large amplitude magnetic disturbances, magnetic filaments, vortices, shocklets, and tangential discontinuities^{14,15} (the list is still not complete).

3. 2D vs 3D coherent structures and magnetic reconnection

Almost all studies on magnetic reconnection so far start with a current sheet already formed in the middle of a 2D periodic simulation box (see Fig. 1)^{16–20}. The problem of CS formation in 3D magnetic topologies and the characteristics of convective flows that drive the reconnection process remained outside the scope of these studies for many years. The evolution of an isolated CS in the presence of weak turbulence in the incoming flows has been analysed recently^{21–24}. The characteristics of the convective flows, which, among others, act as the driver for the reconnection process and are responsible for the breaking of the initial CS and the formation of plasmoids or secondary CSs in 2D numerical simulations, have been analyzed extensively^{18,19,25}.

With the presence of a second CS inside the simulation box, the evolution of magnetic reconnection leads to a multi island environment as well^{26–30}. When starting a simulation with strong turbulence, the CSs appear intermittently at random places inside the 2D periodic simulation box, and their evolution depends on the complex drivers and the CoSs surrounding the reconnecting CSs³¹ (see Fig. 1), and finally, in 3D simulations, the formation of a CS driven by a strongly turbulent surrounding is shown in Fig. 1³². The motion of CoSs also generates waves that are emitted into the ambient plasma.¹¹ Therefore, the intermittent formation of CSs in a 3D strongly turbulent plasma departs radically from the evolution of an isolated CS in 2D, as shown in Fig. 1.

In the early 80’s, the link between reconnection and turbulence has been established²⁷, and a few years later the link between turbulence and reconnection has also been analyzed³³. Several recent reviews discuss the way how turbulence can become the host of reconnecting current sheets and how reconnecting current sheets can drive turbulence^{34–37}. The link between shocks and turbulent reconnection has also been analyzed³⁷.

Strong turbulence and CoSs in the solar atmosphere are driven by the convection zone, and the spontaneous formation of reconnecting and non-reconnecting CSs has been analyzed in several articles^{38–43}.

Our review will focus on the formation and evolution of CoSs inside a 3D strongly turbulent magnetized plasma. In section II, we explore the way how strong turbulence generates CoSs, in section III we analyse the fragmentation and filamentation of a 3D large scale isolated CS, which eventually leads to the formation of a cluster of CoSs and strong turbulence. In section IV, we discuss the presence of strong turbulence and CoSs upstream and downstream of a shock. In Section V, we explore the way how strong turbulence is driven by the convection zone, by emerging magnetic flux, or by unstable large scale magnetic structures in the solar atmosphere. In section VI, we use methods from complexity theory (e.g. Cellular Automata and Self Organized Criticality) to explore the formation and evolution of CoSs (mainly CSs) in a

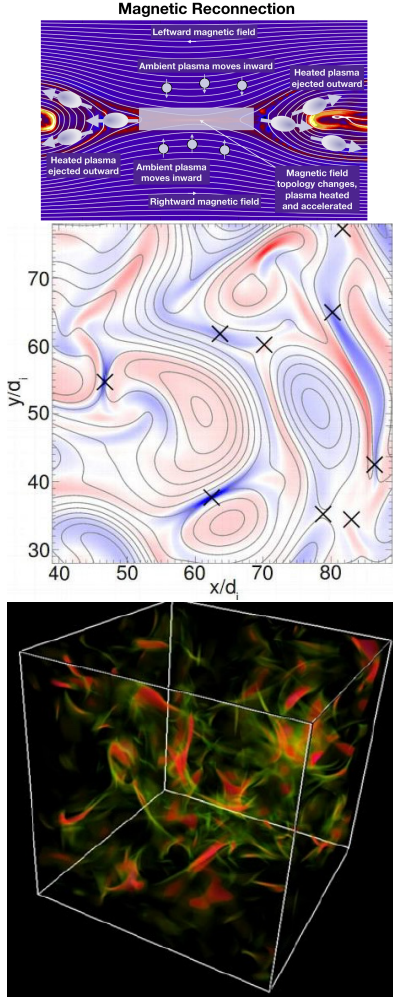


Figure 1. (a) Most numerical studies start with a CS already present in the middle of a 2D periodic simulation box, the driver for the reconnecting CS is either a laminar or “weakly” turbulent flow. Reproduced with permission from Hesse and Cassak, *Journal of Geophysical Research (Space Physics)* **125**, e25935 (2020). Copyright 2020 Wiley. (b) The formation of CSs in 2D strong turbulence is driven by large scale magnetic fluctuations and/or other coherent structures intermittently formed in their vicinity. The CSs are never alone and isolated. The reconnecting sites are marked with crosses and represent a small fraction of the CSs formed. Reproduced with permission from Servidio et al., *Physical Review Letters*, **102** 115003 (2009). Copyright 2009 APS. (c) A snapshot of the spatial distribution of the electric current density in 3D MHD strong turbulence. The formation of 3D CSs is a fundamental aspect of 3D strong turbulence. Reproduced with permission of Minnini et al., *Journal of Plasma Physics*, **73**, 377-401 (2007) Copyright 2007 Cambridge University Press.

strongly turbulent magnetized plasma. In section VII, we summarise the main points of this review.

II. FORMATION OF COHERENT STRUCTURES IN STRONG TURBULENCE

There are several ways to initiate strong turbulence in 2D and 3D numerical simulations^{31,33,37,44–53}. In this section, we follow the approach used initially by Dmitruk et al.⁵⁴ and later by Arzner et al.⁴⁵, Zhdankin et al.⁴⁸ and Isliker et al.⁵¹. In these articles, the authors did not set up a specific geometry of a reconnection environment or prescribe a collection of waves⁵⁵ as turbulence model, but allow the MHD equations themselves to build naturally correlated field structures (which are turbulent, not random) and coherent regions of intense current densities (current filaments or CSs). In this approach, turbulence is freely evolving and ultimately decaying.

The 3D, resistive, compressible and normalized MHD equations used in Isliker, Vlahos, and Constantinescu⁵¹ are

$$\partial_t \rho = -\nabla \cdot \mathbf{p} \quad (2)$$

$$\partial_t \mathbf{p} = -\nabla \cdot (\mathbf{p}\mathbf{u} - \mathbf{B}\mathbf{B}) - \nabla P - \nabla B^2/2 \quad (3)$$

$$\partial_t \mathbf{B} = -\nabla \times \mathbf{E} \quad (4)$$

$$\partial_t (S\rho) = -\nabla \cdot [S\rho\mathbf{u}] \quad (5)$$

with ρ the density, \mathbf{p} the momentum density, $\mathbf{u} = \mathbf{p}/\rho$, P the thermal pressure, \mathbf{B} the magnetic field,

$$\mathbf{E} = -\mathbf{u} \times \mathbf{B} + \eta \mathbf{J} \quad (6)$$

the electric field, $\mathbf{J} = \nabla \times \mathbf{B}$ the current density, η the resistivity, $S = P/\rho^\Gamma$ the entropy, and $\Gamma = 5/3$ the adiabatic index.

In Isliker, Vlahos, and Constantinescu⁵¹, the MHD equations are solved numerically in Cartesian coordinates with the pseudo-spectral method⁵⁶, combined with the strong-stability-preserving Runge Kutta scheme⁵⁷, and by applying periodic boundary conditions to a grid of size $128 \times 128 \times 128$. A fluctuating magnetic field \mathbf{b} consist of a superposition of Alfvén waves, with a Kolmogorov type spectrum in Fourier space, together with a constant background magnetic field B_0 in the z -direction, so the magnetic field used as initial condition is $\mathbf{B} = \mathbf{B}_0 + \mathbf{b}(x, y, z, t)$. The mean value of the initial magnetic perturbation is $\langle b \rangle = 0.6B_0$, its standard deviation is $0.3B_0$, and the maximum equals $2B_0$, so that indeed strong turbulence is considered. The initial velocity field is 0, and the initial pressure and energy are spatially constant.

The structure of the z -component of the current density J_z is shown in Fig. 2 (the threshold value is chosen as the value above which the frequency distribution of the current density values deviates from Gaussian statistics, forming an exponential tail.).

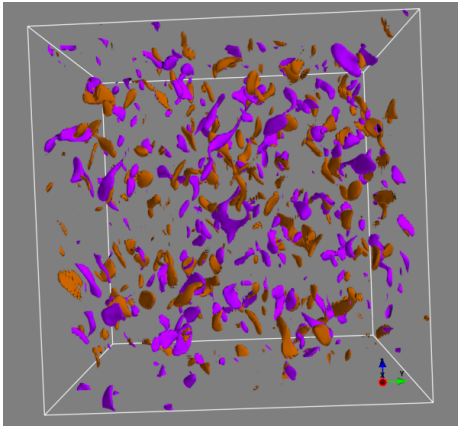


Figure 2. Iso-contours of the supercritical current density component J_z (positive in brown negative in violet). Reproduced with permission from Isliker et al., *Physical Review Letters*, **119**, 045101 (2017), Copyright 2017 APS

For the CoSs to form, Isliker et al.⁵¹ let the MHD equations evolve, until the largest velocity component starts to exceed twice the Alfvén speed. The magnetic Reynolds number at final time is $\langle |\mathbf{u}| \rangle l / \eta = 3.5 \times 10^3$ (being actually rather constant over time), with $l \approx 0.01$ a typical small scale eddy size, and the ratio of the energy carried by the magnetic perturbation to the kinetic energy is $(0.5 \langle b^2 \rangle) / (0.5 \langle \rho \mathbf{u}^2 \rangle) = 1.4$, which is a clear indication that they were dealing with strong turbulence.

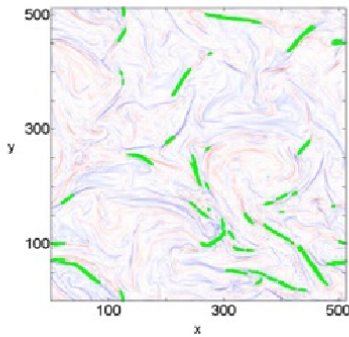


Figure 3. Current density in the cross section of the x - y plane. Red indicates negative current, and blue indicates positive current. The presence of current sheets (in green color) throughout the volume is clearly visible. Reproduced with permission from Zhdankin et al., *The Astrophysical Journal*, **771**, 124 (2013), Copyright 2013 AAS.

The overall picture demonstrates the spontaneous formation of CoSs, with the intermittent appearance and disappearance of CSs dominating the overall evolution of the strongly turbulent environment. This result resembles the 2D simulations of Biskamp and Walter³³ about thirty years ago. The perpendicular component of the current fluctuates rapidly but lacks the coherent structures shown in J_z . Similar results were obtained by Arzner et al.^{45,55}, using strong Gaussian fields or a large

eddy simulation scheme.

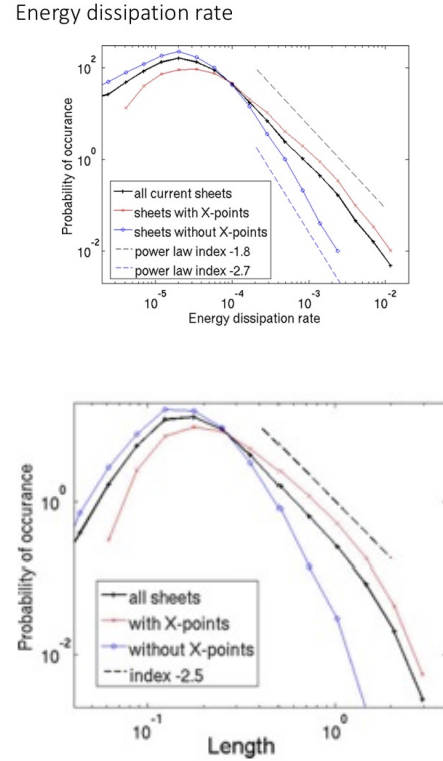


Figure 4. (a) Probability distribution of the current sheet Ohmic dissipation rate. The distribution from all currents sheets shows a power law tail with index close to -1.8 . (b) Probability distribution of the current sheet lengths. Reproduced with permission from Zhdankin et al., *The Astrophysical Journal*, **771**, 124 (2013), Copyright 2013 AAS.

It is of foremost importance to find ways to identify 3D CoSs inside a turbulent plasma and measure their statistical characteristics. Several algorithms have been proposed in order to identify and characterize the geometrical structures of CoSs in numerical simulations and observations^{31,46–48,58–65}.

Dong et al.⁶⁶ presented the world's largest, so far, 3D MHD turbulence simulation, using ~ 200 million Central Processing Unit (CPU) hours. In their analysis, a myriad of fine structures (CSs) is produced (see Fig. 5),

They initialized their simulation with uncorrelated, equipartitioned velocity and magnetic field fluctuations superimposed onto a strong mean magnetic field. Their main focus was on the properties of the reconnection-driven energy cascade, and they also discussed the role that the break up of the reconnecting CSs into smaller fragments plays in the energy transfer. The fragmentation of large scale CSs is the topic of the next section in this review.

Comisso and Sironi⁶⁷ showed that coherent structures (referring mainly to CSs) undergo fragmentation and reconnection in fully kinetic simulations of strong plasma

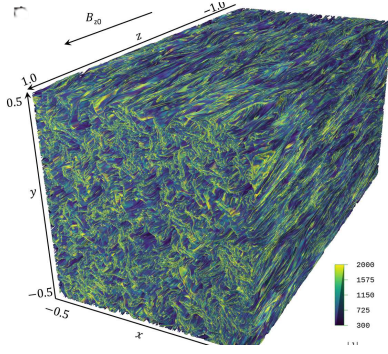


Figure 5. Volume rendering of the current density $|J|$ in the entire domain at a stage when turbulence is fully developed. A myriad of current sheets is evident in the plane perpendicular to the mean magnetic field B_{z0} (for details of the simulation see Dong et al.⁶⁶). Reproduced with permission from Dong et al., *Science Advances*, **8**, 7627 (2022), Copyright 2022 AAAS.

turbulence. Their study proved that reconnecting current sheets are a common feature of not only the MHD models but also of the more complete fully kinetic models.

Zhdankin et al.⁴⁸ developed a framework for studying the statistical properties of CSs formed inside a magnetized plasma by using a 3D reduced MHD code. The distribution of the current fragmentation forming CSs in the x - y -plane is shown in Fig. 3. They were able to show that a large number of CSs do not contain reconnection sites, and likewise, many reconnection sites do not reside inside 3D CSs.

The most striking characteristic of the CSs formed spontaneously inside the strongly turbulent plasma is the probability distribution of the dissipated energy, $\varepsilon = \int \eta j^2 dV$, and of the characteristic lengths of the CSs, which are shown in Fig. 4, as reported by Zhdankin et al.⁴⁸. The techniques applied by Zhdankin et al.⁴⁸ for the analysis of their numerical simulations have initially been developed by Urisky et al.⁵⁹. Recently, a number of attempts were made to extend the search for 3D CoSs to satellite data^{62,64}.

The distribution in real space of CoSs in turbulence influences their dynamics and dissipation characteristics through the complex interrelationship. In Fig. 6, the probability distribution function (PDF) of the electric current density is shown, and corresponding regions in real space are indicated⁵⁸. The low values of the current density (region I) follow a supergaussian distribution and are related with the lanes between the islands. The intermediate values of the current density (region II) correspond to cores (filaments in 3D) and follow a subgaussian distribution, and finally the supergaussian tails of the distribution (region III) with the strongest current densities possibly represent the current sheets between interacting magnetic islands (filaments in 3D).

When confronted with a dataset that samples a turbulent plasma system spatially, an important task is to find the subset of the data that corresponds to the underlying

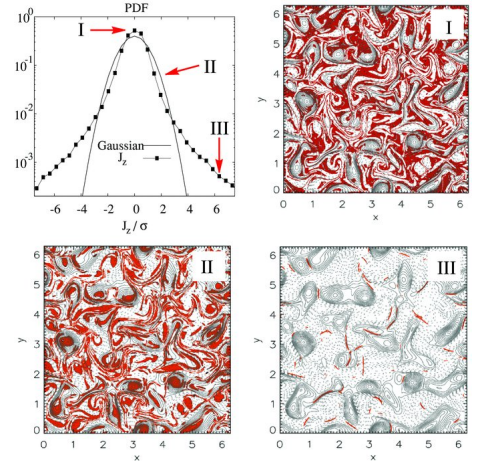


Figure 6. The PDF of the electric current density from 2D MHD simulations. Real space locations belonging to the regimes I, II and III are shown in the other three panels. Reproduced with permission from Greco et al., *The Astrophysical Journal Letters*, **691**, L111 (2009), Copyright 2009 AAS.

CoSs. In recent years, a plethora of methods has been suggested for the identification of intermittent structures and discontinuities in the magnetic field. These include the Phase Coherence Index method⁶⁸ and the wavelet-based Local Intermittency Measure (LIM)⁶⁹. A simple and well-studied method that has been effectively used in the past for the study of intermittent turbulence and the identification of CoSs, both in simulations⁴⁷ and observations^{70,71}, is the Partial Variance of Increments (PVI) method. The advantage of the PVI method is that it provides an easy-to-implement tool that measures the sharpness of a signal relative to the neighborhood of a point. For a lag τ , the normalized PVI at time t is defined as

$$PVI(t, \tau) = \frac{|\Delta \mathbf{B}(t, \tau)|}{\sqrt{\langle |\Delta \mathbf{B}(t, \tau)|^2 \rangle}}, \quad (7)$$

where $|\Delta \mathbf{B}(t, \tau)| = |\mathbf{B}(t + \tau) - \mathbf{B}(t)|$ is the magnitude of the magnetic field vector increments, and $\langle \dots \rangle$ denotes the average over a window that is a multiple of the estimated correlation time. PVI is a threshold method, so to proceed with the analysis, one imposes a threshold θ on the PVI and selects portions in which $PVI > \theta$. Greco et al.⁷² have shown that increments with $PVI > 3$ lie in the “heavy tails” observed in the distribution of increments and can thus be associated with Non-Gaussian structures (see Fig. 6). By increasing the threshold value θ , one can thus identify the most intense magnetic field discontinuities like CSs and reconnection sites. Finally, note that the method is insensitive to the mechanism that generates the coherent structures and it is more general and could be applied to 3D structures as well with appropriate modifications. This means that the PVI can be implemented for the identification of any form of sharp gradients in the magnetic field. A more comprehensive

review of PVI, as well as a comparison with the aforementioned methods, appropriate for identifying discontinuities, can be found in Greco et al.⁷²

The histogram of the frequency of occurrence of PVI values in the solar wind data suggests that the most probable value of PVI is about 0.5 (see Fig. 7), where the majority of nonintermittent events takes place⁷¹. A large number of non-Gaussian ($3 < PVI < 6$) events appear in the histogram in Fig. 7. The percentage of possibly reconnecting events ($PVI > 8$) drops dramatically^{65,71}, suggesting, as we have stressed earlier^{3,48}, that only a small fraction of the detected CSs are actually reconnecting.

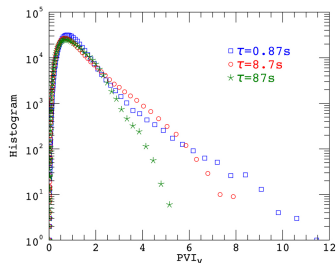


Figure 7. Histograms (frequency of occurrence, or number of counts) of PVI values for different lags τ . Note the elevated likelihood of large PVI values at shorter lags, which is indicative of enhanced small-scale intermittency, typical of non-Gaussian processes and turbulence. Reproduced with permission from Chhiber et al., The Astrophysical Journal Supplement, **246**, 31 (2020), Copyright 2020 AAS.

The techniques to explore the formation and evolution of CoSs at different scales in strongly turbulent magnetized plasma are in their infancy, and novel techniques are needed to understand the statistical properties of CoSs. We just mention that Jiang et al.⁷³ used convolutional neural networks to model strong hydrodynamic turbulence and to follow the formation and evolution of CoSs.

The main focus in most of the studies reported so far was on the presence of intense CSs and especially reconnecting CSs inside the turbulent medium. Only recently the analysis was extended to other types of CoSs⁶³, e.g. vortex-like structures, wave packets, and Alfvénic fluctuations.

Karimabadi et al.³⁷ stress the fact that the motion of CoSs generates waves that are emitted into the ambient plasma in the form of highly oblique compressional Alfvén modes, as well as large amplitude magnetic disturbances. This indicates that strong turbulence will in general consist of CoSs and waves, therefore “weak” and strong turbulence co-exist in the multiscale evolution of a strongly turbulent plasma. Grošelj et al.⁷⁴ explore the very important question of the relative importance of coherent structures and waves in strongly turbulent plasma, utilizing high-resolution observational and simulation data. They investigate the nature of waves and structures emerging in a weakly collisional, turbulent kinetic plasma. Their observational results are based on in situ solar wind measurements from the Cluster and

the MMS spacecraft, and the simulation results are obtained from an externally driven, three-dimensional fully kinetic simulation. Using a set of novel diagnostics described in their article in detail, they show that both the large-amplitude structures and the lower-amplitude background fluctuations preserve linear features of kinetic Alfvén waves to order unity. This quantitative evidence suggests that kinetic turbulence cannot be described as a mixture of mutually exclusive waves and structures, but may instead be pictured as an ensemble of localized, anisotropic wave packets or “eddies” of varying amplitudes, which preserve certain linear wave properties during their nonlinear evolution. This important finding and its role in the energy dissipation in strong turbulence, as well as its role in particle heating, has not been evaluated properly till now.

Large scale magnetic disturbances and CoSs in fully developed turbulence exhibit a monofractal or multifractal structure, both in space and astrophysical plasma^{75–80}. This information is very important for analysing the interaction of particles with CoSs⁸¹.

As we have already stressed, CSs are not the only coherent structures that appear in MHD turbulence. One also finds current cores, vorticity concentrations, and density structures^{82–84}. An informative example of neighboring coherent structures is found in the phenomenon of magnetic reconnection. It involves the formation of current sheets or filaments that become the organizational focus of the reconnection process as a whole. This subtle interplay between coherent structures of different types (magnetic filaments, vortices, small-scale shocks, large amplitude magnetic disturbances) is indicative of the physics that controls the lower end of the MHD/fluid cascade. These CoSs are likely the dominant loci of dissipative processes, not only in fluid models but also in kinetic approaches to plasmas³.

Concerning laboratory plasmas in tokamak devices, we note that turbulence appears predominantly at different spatial and temporal scales throughout the plasma^{85–87}. Microscopic turbulence dominates in the plasma core, and it limits the steepness of the plasma temperature and density profiles⁸⁸. In the plasma edge region, microscopic and fluid turbulence can also be present in a dominant way when the plasma is in the so-called low confinement regime (L-mode). On the other hand, strong suppression of turbulence leads to the formation of a transport barrier and gives rise to the high confinement regime (H-mode), which exhibits a pedestal (extending over the edge transport barrier) that increases the core pressure^{89,90}.

Edge localized modes (ELMs) are violent and transient MHD instabilities that repeatedly take place in tokamak H-mode plasmas and are caused by large current densities and pressure gradients in the pedestal region. ELMs lead to a repeating loss of the plasma confined in the edge region, and particles and heat are lost to the wall on a time scale of $\lesssim 1$ ms^{91–93}. During ELMs, filamentary eruptions are observed, as well as magnetic field stochasticization⁹⁴. Magnetic perturbations during ELMs

are linked to reconnection, since they are the result of resistive peeling-ballooning modes, which trigger magnetic reconnection at the resonant surfaces.

To some degree, ELMS can be viewed as the analog of coronal emerging flux scenarios in laboratory plasmas, and it is worthwhile discussing briefly the commonalities and differences between laboratory and astrophysical plasma eruptions, on the example of ELMS in tokamaks and solar flares.

Both, solar corona and tokamak plasmas, are characterized by an electrical resistivity that is low in the sense that the Lundquist number is much larger than unity if the length scale considered is the macroscopic system size⁹⁵. The macroscopic lengths are also much larger than the kinetic scales (electron and ion Larmor radii) in both systems. The strong toroidal field in tokamaks ensures that the plasma beta $\beta = p/(B^2/2\mu_0)$ (with p the plasma pressure and B the magnetic field) is smaller than unity, as it also holds in the flaring corona. Of course, there are enormous differences in absolute system size and duration of eruptive events, which both are larger by a factor of about 10^7 in flares than in ELMS⁹⁵. Yet, when considering the kinetic scales, which definitely are relevant for particle acceleration and heating, the respective plasma parameters have ratios of solar coronal values to tokamak values rather close to unity^{95,96}.

There is an important topological difference between the two systems. In tokamak plasmas, the magnetic field lines in almost the entire plasma form a set of closed, nested, toroidal surfaces, whereas in flare plasmas, the coronal magnetic field is anchored in the much denser and cooler convection zone. As McClements⁹⁶ notes, there is always an outermost surface of closed magnetic flux in tokamaks, beyond which there is a relatively thin scrape-off layer (SOL) of plasma exhausted from the closed flux region. In most currently operating tokamaks, the magnetic field lines in the SOL are connected to a solid surface at the top or bottom of the vacuum vessel, called divertor. The SOL magnetic field topology thus resembles somehow to that of a flaring coronal loop, with the divertor playing the role of the convection zone. We though note that this is rather an analogy than a one-to-one correspondence, since the divertor is a passive device and does not drive the magnetic field in any way, whereas the convection zone is the main driver and ultimate energy source for coronal magnetic activity, such as flares.

A different, but still qualitative view, is to relate the solar convection zone with the well-confined region within the last closed magnetic surface of a tokamak, and to view the SOL as the analogue of the solar corona, into which ELMS break out from the well-confined region and cause eruptive events, very much like magnetic flux that emerges from the solar convection zone into the solar corona and leads to destabilization and eventually to explosive events, such as flares. In this view, turbulence in the well confined region of a tokamak and in the solar convection zone have in common to be the driver of the eruptive events, ELMS and flares, respectively.

Isliker *et al.*⁹⁷ presented test-particle simulations of electrons during a nonlinear MHD simulation of an ELM. Their aim was to explore the effect of an eruptive plasma filament on the particle dynamics. They found that the electrons are moderately heated and accelerated during the ELM, on a fast time scale of the order of 0.5 ms. Also, the distribution of the kinetic energy exhibits a non-thermal tail, which is of power-law shape, reaching up to 90 keV. The acceleration exclusively takes place in the direction parallel to the magnetic field, and they showed that the parallel electric field is the sole cause of the particle acceleration. Most particles that escape from the system leave at one strike-line in the bottom region of the device (the outer divertor leg). The escaping high energy electrons in the tail of the energy distribution have characteristics of runaway electrons. The mean square displacement in energy space indicates that transport is super-diffusive, and, when viewing the acceleration process as a random walk, they found that the tails of the distributions of energy increments are of exponential shape. They also noted that transport in energy space is equally important of diffusive (stochastic) and convective (systematic) nature.

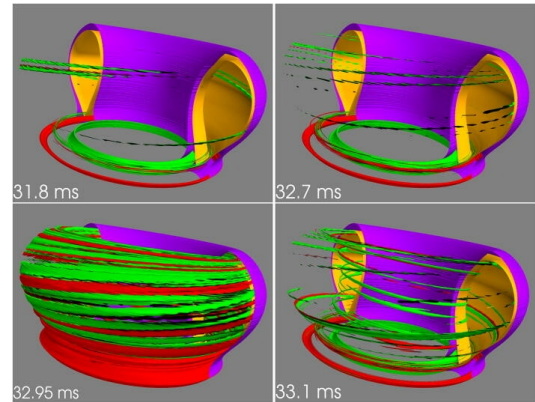


Figure 8. Iso-contours of the parallel electric field E_{\parallel} (positive at +10 V/m in red, and negative at -10 V/m in green), for four different times during the ELM, together with the separatrix (orange) and the plasma-boundary (violet) (both surfaces are half cut out). Reproduced with permission from Isliker *et al.*, *Physics of Plasmas*, **29**, 124 (2022), Copyright 2022 AIP.

Isliker *et al.* also analyzed the MHD simulations *per se* (see Fig. 8), with the main finding that the histograms of the parallel electric field in the edge region adopt power-law shapes, and they concluded that this clearly non-Gaussian statistics is one of the main reasons for the moderately anomalous phenomena of particle transport in energy space that they find.

Solar wind⁹⁸, the Earth's magnetosheath^{99,100}, astrophysical jets^{52,101,102}, and edge localised turbulence in tokamaks⁸⁷ are only a few space and laboratory examples of CoSS formation in strongly turbulent plasmas.

III. FORMATION OF COHERENT STRUCTURES FROM THE FRAGMENTATION OF LARGE SCALE CURRENT SHEETS

The formation and fragmentation of large scale CSs in many space and astrophysical settings are worthwhile being studied in detail, as we will see at the end of this section. The fragmentation of an isolated large scale CS in 2D magnetic topologies, with the formation of plasmoids during the linear phase of the plasmoid instability, has been analysed extensively^{103,104}. Our main interest here is though in the 3D evolution and fragmentation of CSs in strongly turbulent environments.

Matthaeus and Laskin²⁷ were the first to move away from the laminar reconnection flows and to explore the evolution of a 2D periodic CS in the presence of low level broadband fluctuations. It is worthwhile quoting the main findings from the abstract of their seminal article with the title “*Turbulent magnetic reconnection*”: “*Nonlinear features of the evolution, appropriately described as turbulence, are seen early in the solutions and persist throughout the runs. Small scale, unsteady coherent electric current and vorticity structures develop in the reconnection zone, resulting in enhanced viscous and resistive dissipation. Unsteady and often spatially asymmetric fluid flow develops. Large scale magnetic islands, produced by reconnection activity, undergo internal pulsations. Small scale magnetic islands, or bubbles, develop near the reconnection zone, producing multiple X points. Large amplitude electric field fluctuations, often several times larger than the reconnection electric field, are produced by large island pulsations and by motion of magnetic bubbles. Spectral analysis of the fluctuations shows development of broad band excitations, reminiscent of inertial and dissipation range spectra in homogeneous turbulence. Two dimensional spectra indicate that the turbulence is broadband in both spatial directions. It is suggested that the turbulence that develops from the randomly perturbed sheet bears a strong resemblance to homogeneous magnetohydrodynamic turbulence, and that analytical theories of reconnection must incorporate these effects.*”

Lazarian and Vishniac²¹ returned to the formation of a CS in the middle of weakly turbulent flows (see their cartoon in Fig. 9). They generalised the results of Matthaeus and Laskin²⁷, using a 3D magnetic topology, and stressed the importance of stochastic magnetic field wandering, which causes fragmentation of the initial large scale astrophysical current sheet. The reconnection in small fragments of the magnetic field determines the local reconnection rate and the local strength of the electric field. The global reconnection rate is substantially larger, as many independent fragments reconnect simultaneously. Lazarian and Vishniac also obtained quantitative predictions for the reconnection rate (see details in Lazarian *et al.*¹⁰⁵).

Onofri *et al.*^{106,107} numerically solved the incompressible, dissipative, magnetohydrodynamics (MHD) equa-

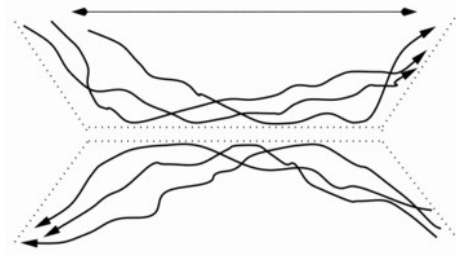


Figure 9. The Lazarian and Vishniac model²¹ for a 3D weakly turbulent reconnection driver. The width of the outflow can be compatible with the large scale characteristic of the turbulence due to stochastic wandering of field lines and the fragmentation of the initial current sheet. Reproduced with permission from Lazarian and Vishniac, *The Astrophysical Journal*, **517**, 700 (1999), Copyright 1999 AAS.

tions in dimensionless units in a three-dimensional Cartesian domain, with kinetic and magnetic Reynolds numbers $R_v = 5000$ and $R_M = 5000$. They set up the initial condition in such a way as to have a plasma that is at rest, in the frame of reference of the computational domain, permeated by a background magnetic field sheared along the \hat{x} direction, with a current sheet in the middle of the simulation domain. They perturb these equilibrium fields with three-dimensional divergenceless large amplitude fluctuations. (For details about this MHD simulation see Onofri *et al.*¹⁰⁶.)

The nonlinear evolution of the system is characterized by the formation of small scale structures, especially on the lateral regions of the computational domain, and coalescence of current filaments in the center. This behavior is reflected in the three-dimensional structure of the electric field, which shows that the initial equilibrium is destroyed by the formation of current filaments. After about $t = 50\tau_A$ (where τ_A is the Alfvén time), the current sheet starts to be fragmented, as can be seen in Fig. 10, where we show the configuration of the electric field $\mathbf{E} = \eta\mathbf{J} - \mathbf{v} \times \mathbf{B}$, calculated from the MHD simulation data. The iso-surfaces of the electric field in Figure 10 are shown for different times, and they are calculated for two different threshold values of the electric field: the red surfaces represent higher values and the blue surfaces represent lower values. The structure of the electric field is characterized by small regions of space where the field is stronger, surrounded by larger volumes occupied by lower electric field values. At later times, the fragmentation is more evident, and at $t = 400\tau_A$, the initial current sheet has been completely destroyed and the electric field is highly fragmented. To give a measure of the fragmentation of the electric field, Onofri *et al.*¹⁰⁷ calculated the fractal dimensions of the fields shown in Fig. 10, using the box counting definition of fractal dimension. The applied thresholds are the same as those that have been used to draw the isosurfaces shown in Fig. 10. For the fields represented by the blue surfaces in Fig. 10, they found fractal dimensions $d = 2$, $d = 2.5$, and $d = 2.7$ at

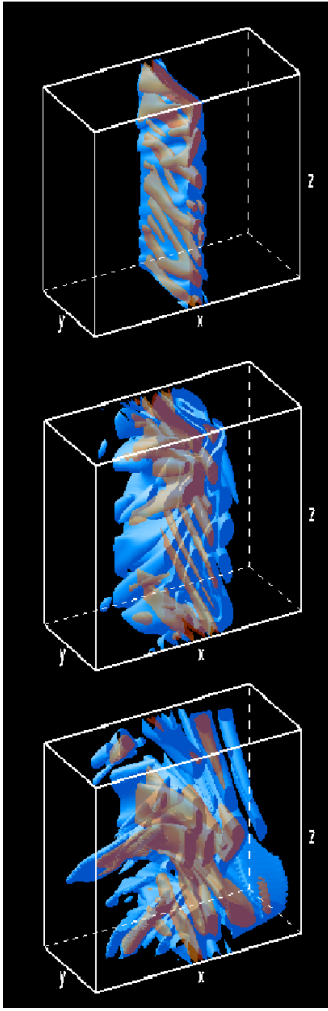


Figure 10. Electric field iso-surfaces at $t = 50\tau_A$, $t = 200\tau_A$ and $t = 400\tau_A$. Reproduced with permission from Onofri et al., *Physical Review Letters*, **96**, 151102 (2006), Copyright 2006 APS.

$t = 50\tau_A$, $t = 200\tau_A$, and $t = 400\tau_A$, respectively. For the more intense electric fields (red surfaces in Fig. 10), the fractal dimensions are $d = 1.8$, $d = 2$, and $d = 2.4$ at $t = 50\tau_A$, $t = 200\tau_A$, and $t = 400\tau_A$, respectively. These fractal dimensions can be considered as a way to quantify the degree of fragmentation of the electric field and to characterize the fraction of space that it fills as it evolves in time.

Onofri et al.¹⁰⁷ calculate the magnitude $|\mathbf{E}|$ of the electric field at each gridpoint of the simulation domain and construct the distribution function of these quantities, which is shown in Fig. 11 for $t = 50\tau_A$. They separately plot the resistive and the convective component of the electric field. The resistive part is less intense than the convective part, but it is much more important in accelerating particles¹⁰⁷.

The fragmentation of a large scale CS was analysed by several authors^{30,108–113}. Dahlin et al.¹¹², using kinetic simulations of 3D collisionless plasma with a guide field,

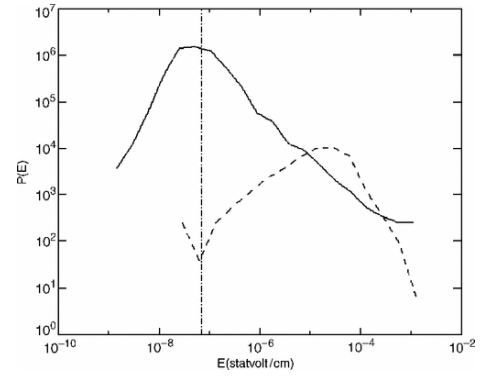


Figure 11. Distribution function of the resistive (solid line) and convective (dashed line) electric field at $t = 50\tau_A$. The vertical line represents the value of the Dreicer field in the solar corona. Reproduced with permission from Onofri et al., *Physical Review Letters*, **96**, 151102 (2006), Copyright 2006 APS.

analyze the fragmentation of a current sheet and the formation of small scale filaments with strong electric fields. A different mechanism to reach the fragmentation of a large scale CS is the presence of other CoSs in the surrounding of the CS, e.g. multiple reconnection sites¹¹⁴.

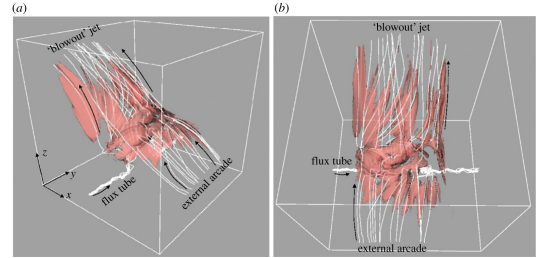


Figure 12. Side-view (panel (a)) and top view (panel (b)) of the 3D field line topology and the velocity during the blowout jet emission. The direction of the field lines is shown by black arrows. Reproduced with permission from Archontis et al., *The Astrophysical Journal Letters*, **769**, L21 (2013), Copyright 2006 AAS.

Greco et al.¹¹⁵, using Cluster high-resolution data, investigated the structure of thin current sheets that populate the turbulent solar wind. They concluded that in the solar wind, the turbulent cascade naturally forms current sheets at several scales, down to the proton skin depth scale. When approaching smaller scales, a current fragmentation process arises.

Beg et al.¹¹⁶ analyzed the formation and evolution of a large-scale CS with a 3D MHD simulation of two merging flux ropes. They discovered that these systems exhibit self-generated and self-sustaining turbulent reconnection, which is fully 3D and fast.

Heyvaerts et al.¹¹⁷ suggested that magnetic flux emerging from below the photosphere and interacting with overlying magnetic fields, forms a quasi static large scale CS that may trigger a solar flare. Several numerical studies further explore the idea of the formation of a large

scale CS from emerging magnetic flux^{118–126}.

Archontis and Hood¹²⁷ used a 3D resistive MHD code to follow the emergence of new magnetic flux into the corona with a pre-existing magnetic field. The formation and subsequent fragmentation of the large-scale reconnecting current sheets is obvious in their numerical study (see Fig. 12).

Islaker et al.⁸⁰ used the 3D MHD simulations of Archontis & Hood¹²⁷, but focused on the statistical properties of the electric fields in the vicinity of the fragmented large-scale current sheet. The appearance of current fragmentation is apparent at the snapshots following the formation of the jet (see Fig. 13). The parallel electric field shows fragmented structures and has preferred regions of positive and negative sign. The fragmentation needs to be quantified with the use of cluster analysis and fractal dimension estimate.

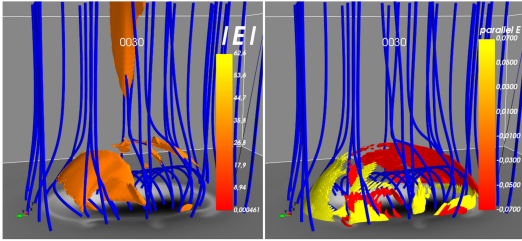


Figure 13. Results from the MHD simulations: a close-up of the coronal part. The left panel shows a visualization of selected magnetic fieldlines (blue) together with an isosurface plot of the total electric field (orange 3D isosurfaces). The vertically oriented isosurface (orange) is aligned with the direction of the reconnected fieldlines and it indicates the emission of the standard jet. The x y -plane at the bottom shows the photospheric component B_z as a 2D filled contour plot. The electric field is in physical units [V m^{-1}]. In the right panel, isocontours of the parallel electric field are shown, indicating the fragmentation of the current sheet at the interface between the interacting magnetic fields. Reproduced with permission from Islaker et al., *The Astrophysical Journal*, **882**, 57 (2019), Copyright 2019 AAS.

Fig. 14 shows the histogram of the magnitude of the total electric field $|\mathbf{E}|$, the parallel $|E_{\parallel}|$, and the perpendicular E_{\perp} component of the electric field, determined from all coronal grid points. They all show a power-law tail with a rollover at high values. The power-law index of the fit is -1.8 for the parallel electric field, and -2.4 for the total and the perpendicular electric field, just that the total and perpendicular electric field attain larger values. In any case, the parallel electric field is two orders of magnitude smaller than the total electric field, which thus basically coincides with the perpendicular electric field. Also, the parallel electric field shows a much more extended power-law tail than the perpendicular and the total one. Islaker et al.⁸⁰ conclude that power-law-shaped distributions are inherent to the electric field and its components. Similar results have also been found in MHD simulations of a decaying current sheet, as we reported earlier in this section (see Fig. 11).

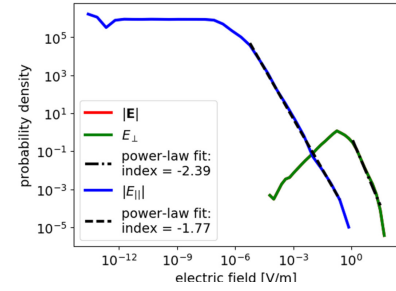


Figure 14. MHD simulations, coronal part only, showing the distribution of the electric field from all coronal grid points, for the magnitude of the total electric field, the perpendicular component (they practically coincide), and the parallel component, respectively. The electric field is in units [V m^{-1}], and the mean Dreicer field is $4.6 \times 10^{-4} \text{ V m}^{-1}$. Reproduced with permission from Islaker et al., *The Astrophysical Journal*, **882**, 57 (2019), Copyright 2019 AAS.

Islaker et al.⁸⁰ also investigate the spatial structure of the parallel electric field, applying cluster analysis and calculating its fractal dimension. They consider the magnitude of the parallel electric field $|E_{\parallel}|$ at all coronal grid points, and apply a threshold below which $|E_{\parallel}|$ is set to zero. For the threshold, they use the same value of 0.07 as for the isocontours of E_{\parallel} in Fig. 13. They define a cluster as a set of grid points with (a) an above-threshold value of $|E_{\parallel}|$ at all the grid points belonging to the cluster, and (b) the cluster's grid points are connected through their nearest neighborhoods in 3D Cartesian coordinates. It follows that a cluster is surrounded by grid points with below-threshold $|E_{\parallel}|$. They found that there are 162 clusters, and 2 of them are very dominant in spatial extent, one corresponding to the positive and one to the negative extended parallel electric field region in Fig. 13. Using the same data as employed in the cluster analysis (the magnitude of the parallel electric field $|E_{\parallel}|$ at all the coronal grid points, set to zero when below the threshold value of 0.07), Islaker et al.⁸⁰ apply a standard 3D box-counting method in order to determine the fractal dimension D_F of the region with above-threshold parallel electric field. Fig. 15 shows the scaling of the box counts with the box scale, where there is a clear power-law scaling in the entire range, whose index, per definition of the box-counting method, equals the fractal dimension, so they find $D_F = 1.7$ for snapshot 30 (standard jet) and $D_F = 1.9$ for snapshot 53 (blowout jet).

The regions of high parallel electric field can thus be interpreted as thinned out 2D sheets, as it also corresponds to the visual impression that is given by Fig. 13. Also, the "filling-factor" (fractal dimension) is higher at the blowout jet compared to the time when the standard jet is emitted. After all, the spatial structure of the regions of strong parallel electric field can be characterized as fragmented and fractal, with the various cluster-size distributions exhibiting double power-law scalings.

The formation of large scale 3D CSs in the middle of converging strongly turbulent flows is present in sev-

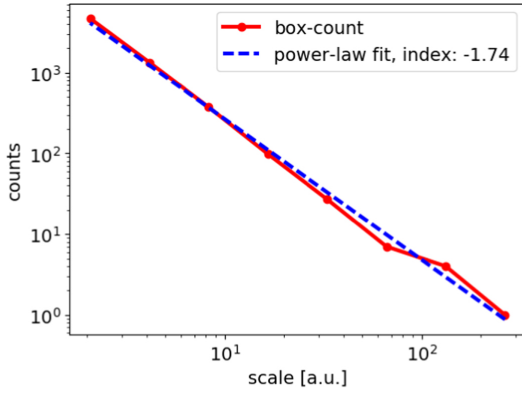


Figure 15. Fractal dimension of the parallel electric field: scaling of the 3D box-counting algorithm. Reproduced with permission from Isliker et al., *The Astrophysical Journal*, **882**, 57 (2019), Copyright 2019 AAS.

eral space and astrophysical phenomena, e.g. the (turbulent) magnetotail¹²⁸ driven by the turbulent solar wind, the (turbulent) magnetopause¹²⁹ driven by the turbulent magnetosheath, eruptive solar flares (resulting from emerging magnetic flux^{127,130}, or from the eruption of large scale magnetic topologies^{131–133}), and the outer heliosphere¹¹⁴. In all these cases, the fragmentation of the CS and its replacement with a much larger strongly turbulent region has led observers to report as a CS the relatively large scale 3D region where the CS's fragmentation was initiated by CoSs included in the 3D magnetic topology of randomly wandering magnetic field lines²¹.

IV. FORMATION OF COHERENT STRUCTURES IN THE VICINITY OF LARGE SCALE SHOCKS

The theoretical analysis of large scale 2D quasi-static shock waves followed, for many years, the same steps as deployed in the large scale Sweet-Parker model for CSs¹⁶. A shock discontinuity was placed by hand in the middle of the simulation box, and weak turbulence was added upstream and downstream, to play the role of converging passive scatterers, since the energization of particles is due to their crossing of the shock discontinuity¹³⁴ (see Fig. 16). The formation of the shock and the way the specific normal modes were excited were not discussed in the initial model proposed by Fermi in 1954¹³⁵, whose approach was used as the base for the subsequent theoretical studies¹³⁶. In this simplistic scenario, the low amplitude wave modes are hand picked carefully to be able to scatter efficiently the particles. The particles, in order to interact with the waves upstream and downstream, should have initial velocity higher than the phase velocity of the wave. This is the well known injection problem, for which a pre-acceleration mechanism is necessary¹³⁶.

Finally, weak turbulence upstream of a shock cannot confine efficiently the accelerated particles in the vicinity of the shock. It was then proposed that streaming

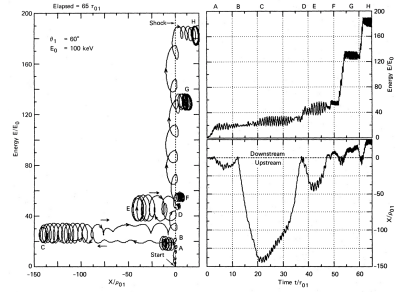


Figure 16. Sample orbit for a quasi-perpendicular shock ($\theta = 60^\circ$). Left: Energy vs. X in the shock frame, where X is the distance from the shock ($X < 0$ upstream; $X > 0$ downstream). Right: Evolution of the energy (upper panel) and of the X -component of the particles position (lower panel) as a function of time. See details in the article Decker and Vlahos¹³⁷. Reproduced with permission from Decker and Vlahos, *The Astrophysical Journal*, **306**, 710 (1986), Copyright 1986 AAS.

instabilities, driven by energized particles upstream of a shock, can be the solution for the trapping of particles in the vicinity of a shock^{138,139}.

Obviously, the formation and evolution of large scale shock waves in space and astrophysical explosions encounter pre-existing or self-generated strong turbulence (e.g. the Earth's and planetary bow shocks in the solar wind, or the shocks formed by Coronal Mass ejection in the heliosphere, or the Super Nova (SN) explosions in astrophysical plasmas). The strongly turbulent plasma upstream of a large scale shock carries a variety of CoSs, which interact with the shock and play a crucial role in its evolution¹⁴⁰. When CoSs cross a shock discontinuity, they are amplified dramatically (see^{37,129,141–147} for the magnetosheath, and the references therein), and the shock surface shows large scale ripples¹⁴⁸.

The Earth's bow shock is the most studied environment of a collisionless large scale shock due to the availability of *in situ* data. The turbulent solar wind upstream carries several types of CoSs (CSs, Cavitons, Rotational Discontinuities (RDs), Short Large Amplitude Magnetic Structures (SLAMs), etc., see Fig. 17), and the instabilities excited by the solar wind ions, reflected at the shock front, re-inforce the unstable CoSs before they are convected downstream^{141–145,149–151}.

Karimabadi et al.³⁷ use a global hybrid simulation (electrons as fluid, kinetic ions) to explore the formation of CoSs in the vicinity of the bow shock. They analyze the link of large scale shock waves, turbulence upstream and downstream, and CoSs. The solar wind turbulence upstream can easily reach the strongly turbulent level ($\delta B/B \approx 1$) and drive turbulent reconnection and the formation of large scale low frequency electromagnetic waves that are compressed and amplified as they cross the shock.

Matsumoto et al.¹⁵² presented a supercomputer particle in cell (PIC) simulation, showing that strong collisionless shocks drive CoSs in the transition region (see

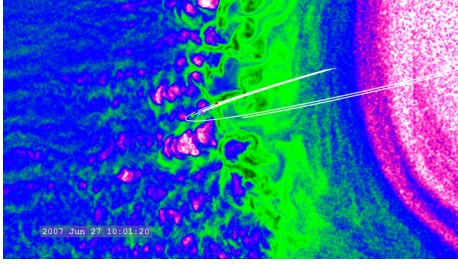


Figure 17. The five THEMIS satellites moving along their orbits. The 2-D data from the Omid simulation¹⁴¹ are faded in and a zoom is made in to a view of the satellites in the turbulent region near the bow shock. The 'cavities' of violet and white color illustrate a broad range of CoSs in this turbulent fore-shock region. Reproduced with permission from Omid, AIP Conference Series, **932**, 181 (2007), Copyright 2007 AIP.

Fig. 18a). They use high computational capacity to follow the evolution of a collisionless shock moving with Mach number $M_A \approx 40$. In Fig. 18a, between the upstream region $x > 59$ and the downstream region $x < 39$, a transition region is characterized by tangled magnetic field lines. This region is in the strongly turbulent state, and the shock front cannot be visually identified. The fragmentation of the shock front drastically modified the assumptions that are behind the analytical work and the simplistic models for diffusive shock acceleration^{153,154}.

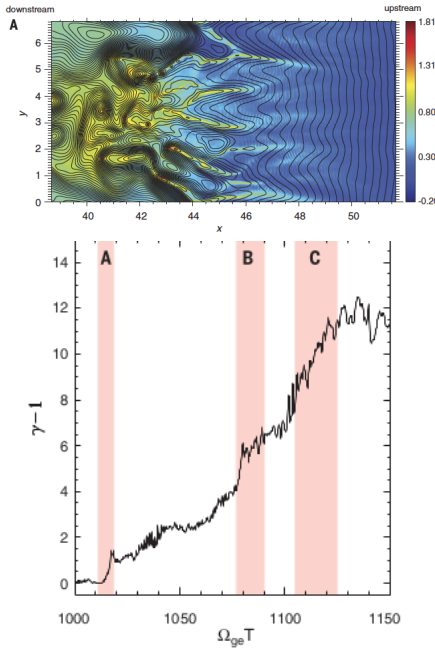


Figure 18. (a) Supercomputer simulation of a strong collisionless shock, revealing the presence of CoSs. (b) An electron's kinetic energy ($\gamma - 1$) as a function of time (normalized to the upstream electron gyro frequency). The times from (A) to (C), for which the particle's orbit is marked, indicate its interaction with specific CoSs downstream (see details in Matsumoto et al.¹⁵²). Reproduced with permission from Matsumoto et al., Science, **347**, 974 (2015), Copyright 2015 AAAS.

It is also of interest to note that filamentary structures are created, as can be seen from the density profile in the transition region in Fig. 18a. These filaments are associated with folded magnetic field lines, and the enhanced density regions contain CoSs. Matsumoto et al.¹⁵² also observe that magnetic reconnection takes place at multiple sites, and, as a result, magnetic filaments are formed along the initial current sheet. Fig. 18b presents the evolution of the kinetic energy of a particle, which shows enhanced gains in energy during the interactions with specific CoSs downstream. Similar evidence for magnetic reconnection is found in other current sheets in the transition and the downstream region¹⁵². This fragmentation of the initial large scale shock front is reminiscent of the large scale CS fragmentation discussed in Sec. III. Similar results are reported by Caprioli and Spitkovsky¹⁵⁵ by using 3D hybrid simulations.

Korpotina et al.¹⁴⁵ analysed the interaction of CoSs (in their case they focused on rotational discontinuities) carried by the turbulent solar wind with the Earth's Bow shock. They used *in situ* multispacecraft observations and performed hybrid kinetic simulations. In their article, they stress the amplification of the CoSs in the vicinity of the shock discontinuity. The amplification of the CoSs carried by the solar wind may be as high as two orders of magnitude. The amplification in the foreshock may be due to streaming instabilities, driven by the interaction of the solar wind with reflected solar wind particles. The Earth's bow shock crossing affects the CoSs, since downstream of the shock the magnetic field and the plasma density are amplified (actually, the observed compression ratio far exceeds the Hugoniot prediction; see also the recent study by Trotta et al.¹⁵⁶). Guo et al.¹⁵⁷, using a 3D global hybrid simulation, showed that the upstream turbulence at a quasi-parallel shock may intensify the presence of CoSs at the rate of reconnection at the magnetosheath downstream of the Earth's bow shock (similar results are reported in several recent articles^{129,142-144,146,147}).

Unfortunately, the multi-scale character and the complexity of the microphysics¹⁴⁰ present in an evolving large scale shock cannot be explored by current numerical simulations, and neither can they follow a shock's evolution for long time. This is the main reason why we are still missing many important details on the evolution of CoSs and their role in the heating and acceleration of particles.

The topic of the interaction of large scale shocks with plasma turbulence and the formation of CoSs upstream and downstream as well as the non-stationary evolution of a 3D shock discontinuity¹⁴⁸ is currently an open problem in space and astrophysical plasmas. Moreover, the collective interaction of particles with the rich variety of CoSs (and not only the reconnecting CSs) and its effect on the heating and acceleration of particles also remain an open problem.

V. FORMATION OF COHERENT STRUCTURES IN THE SOLAR ATMOSPHERE

In the solar atmosphere, CoSs are formed through the strong magnetic coupling with the turbulence in the convection zone. We can split our presentation of the formation of CoSs in the solar atmosphere in two parts: (1) The formation of CoSs by the random shuffling of the footpoints of the slowly changing magnetic fields, and (2) the formation of CoSs during the emerging magnetic flux and/or the large scale magnetic eruptions.

1. Formation of CoSs in quasi-static closed magnetic topologies

In the solar atmosphere, the formation of CoSs (in the cited literature the emphasis is on the formation and disruption of current sheets) through small scale random shuffling of the footpoints of emerged magnetic fields, caused by the convection zone, was first proposed by Gold¹⁵⁸ in the 60s as the main mechanism for coronal heating. The initial conjecture was developed further in the 70s and the 80s^{38,159–162}, and it continues till today, as we will show in this section. Based on this scenario, Parker³⁹ introduced the concept of nanoflares for the formation and disruption of small scale current sheets (Glencross¹⁶⁰ defined the same phenomenon as “flare-like” brightenings, and several years later Chiuderi¹⁶³ called the same phenomenon “elementary events”) as the main mechanism for coronal heating. In other words, the formation of small scale CSs and their collective Ohmic dissipation in closed magnetic topologies is widely accepted as a potential mechanism for coronal heating today. In Fig. 19, we present a cartoon showing the magnetic coupling of the turbulent convection zone with the solar atmosphere above an active region. The details of the formation of the CoSs through the interaction of the solar atmosphere with the turbulent convection zone remain an open problem till today.

In the beginning of the nineties, it was shown that the peak-luminosity distribution of flares displays a well-defined, extended power law with index -1.7 to -1.85 , see Fig. 20¹⁶⁴. This analysis was repeated and confirmed by several authors over the last thirty years (see the reviews^{165,166}).

Deviations from the power law behavior appear at the lowest energies. It has been pointed out that these deviations are due to instrumental limitations. The interesting part from the statistical analysis of solar flares is that the power-law is extended to all flare energies (from micro flares with energies around 10^{24} erg to flares with energies 10^{30} erg). The magnetic link of the turbulent driver (convection zone) with the solar atmosphere is probably behind the statistical properties of the energy release in closed magnetic topologies and can serve as a test for the numerical simulations that will be presented in this section.

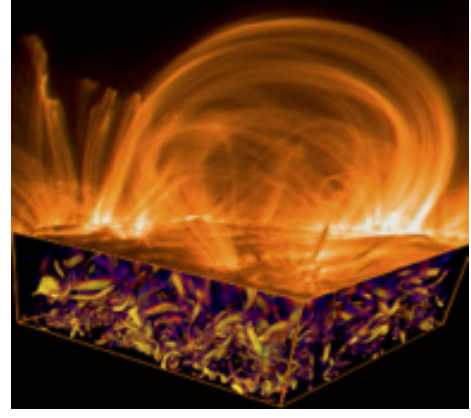


Figure 19. The magnetic link of the convection zone with the solar corona: The turbulent convection zone drives the formation of CoSs in the closed magnetic topologies above the the photosphere.

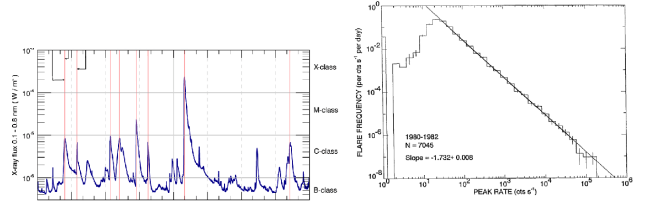


Figure 20. (a) A typical solar X ray flux from February 14, 2011 till February 15, 2011. (b) The frequency distribution of the peak count rate for the flares recorded in 1980-1982. Reproduced with permission from Grosby, Non-linear Processes in Geophysics, **18**, 791 (2011), Copyright 2011, Licensed under Creative Commons Attribute (CC-BY).

In the 90’s, the conjecture reported above for the formation of CSs in solar active regions, through random shuffling of the footpoints of closed magnetic fields, was tested by using 2D and 3D numerical MHD codes^{40–43,167–175}.

Einaudi et al.¹⁶⁸ analyzed a 2D section of a coronal loop, subject to random forcing of the magnetic fields. The title of their article was “Energy release in a turbulent corona”, and they discussed the spontaneous formation of current sheets. Georgoulis et al.¹⁶⁹ extended the simulation of Einaudi et al. for much longer times, since their aim was to extract reliable statistical information on turbulent reconnection in the solar atmosphere. Their main result was that the distribution functions of both the maximum and average current dissipation, for the total energy content, the peak activity and the duration of such events are all shown to display robust scaling laws. This result was recovered by the analysis performed twenty years later by Zhdankin *et al.*⁴⁸, which is briefly reported in section II.

Galsgaard and Nordlund^{40–42} solved the dissipative 3D MHD equations in order to investigate the formation of CSs inside an initially homogeneous magnetic flux tube, stressed by large scale sheared random motions at the

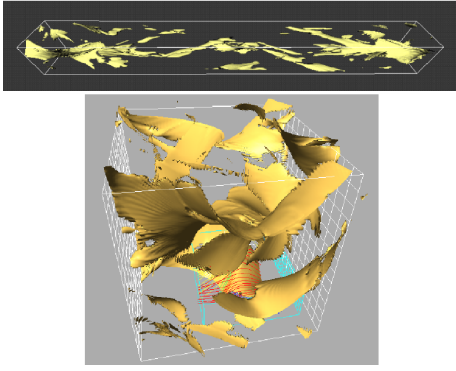


Figure 21. (Top) Isosurfaces of Joule dissipation regions inside a solar magnetic loop driven by random shuffling of the footpoints. (Bottom) Isosurfaces of strong electric currents in a snapshot. Reproduced with permission from Galsgaard and Nordlund, *Journal of Geophysical Research*, , **101**, 13445 (1996), Copyright 1996 Wiley.

two boundaries. The spontaneous formation of CSs at random places at random times inside the structure is shown in Fig. 21. CSs of all scales appear and evolve since the large scale CSs fragment, as we have shown in section III.

Reconnection of the current sheet(s) will straighten the field lines, but will also cause disturbances in the surrounding plasma, causing further fragmentation of the energy release processes. A strongly turbulent environment is established inside the magnetic flux tube, driven by the random shear caused by photospheric motions and by the energy delivered into the solar corona through the dissipation of fragmented current sheets (see similar results in^{107,112}). The evolution of the CoSs depends on the velocities of the boundary motions and the initial magnetic field strength in the magnetic flux tube.

Turkmani et al.^{176,177} analyzed the statistical properties of the electric fields inside the flux tube studied by Galsgaard and Nordlund^{40,41}. The magnetic and electric fields are obtained from a 3-D MHD experiment that represents a coronal loop with photospheric regions at both footpoints. Photospheric footpoint motion leads to the formation of a hierarchy of current sheets, see Fig. V 1a. The distribution function of the resistive electric field has a power law tail for the super-Dreicer electric fields, with slope -2.8 (see Fig. V 1b), and this finding is analogous with the results reported in other studies related with the fragmentation of a large scale CS^{80,107}.

In a series of articles, Rappazzo et. al.^{170,178–180}, following the steps of the work of Galsgaard and Nordlund⁴⁰, analyzed several aspects of the formation of CSs in the solar corona (see Fig. 23). The observational expectations of intermittent energy dissipation in the formed and fragmented CSs were also analyzed in depth^{43,172}.

The numerical simulations presented so-far were performed, for the sake of simplicity, in isolated magnetic flux tubes.

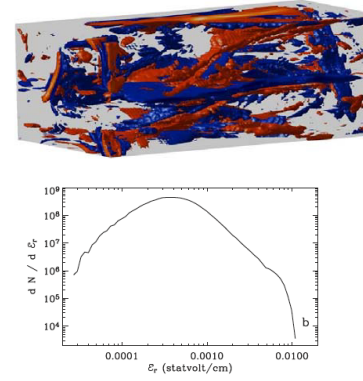


Figure 22. (a) Snapshot of the resistive electric field configuration within the coronal volume, as calculated from the global MHD model. The blue and red regions represent electric field regions that point towards the left and right footpoint, respectively. (b) The distribution function of the resistive electric field. Reproduced with permission from Turkmani et al., *Astronomy and Astrophysics*, **449**, 749 (2006), Copyright 2006 ESO.

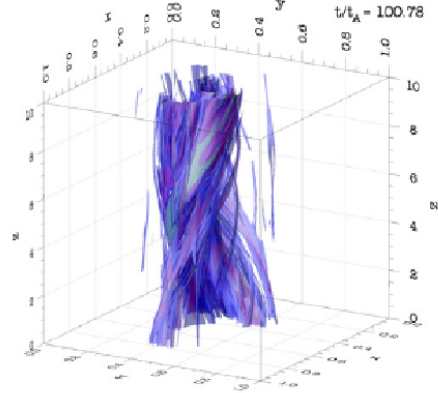


Figure 23. Isosurfaces of the squared current j^2 at a time after the start of the kink instability. Reproduced with permission from Rappazzo et al., *The Astrophysical Journal*, **771**, 76 (2013), Copyright 2013 AAS.

Threlfall et al.¹⁸¹ analyzed the evolution of multi-threaded coronal magnetic flux tubes (see Fig. 24), which become unstable when varying the driving velocity of the individual threads. Assuming that one of the threads is destabilized, it will very quickly lead the system of threads to a strongly turbulent environment, forming many CoSs of different scales, and it reorganizes the multi-threaded topology into a complex magnetic topology with several multi scale intermittently appearing and disappearing current filaments (Fig. 25) (see details in Threlfall et al.¹⁸¹ and references therein).

Archontis and Hansteen¹⁸² reported on the formation of CoSs generated by patchy magnetic reconnection between interacting magnetic loops as well, using a different initial setup. A three-dimensional magnetohydrodynamic numerical experiment was performed, where a uniform magnetic flux sheet was injected into a fully devel-

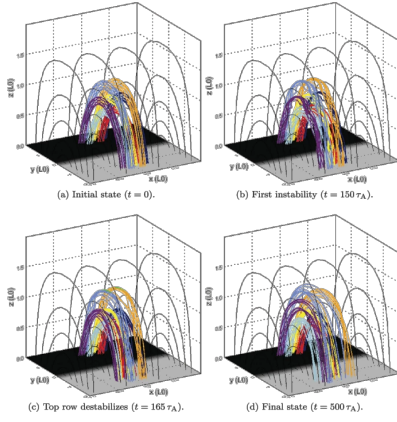


Figure 24. Seven threads with identical drivers: 3D magnetic configuration at different times. When one of the threads is destabilised, it interacts with the rest of the threads and destabilizes all of them, causing the formation of several CoSs. Reproduced with permission from Threlfal et al., *Solar Physics*, **296**, 120 (2021), Copyright 2021 Springer

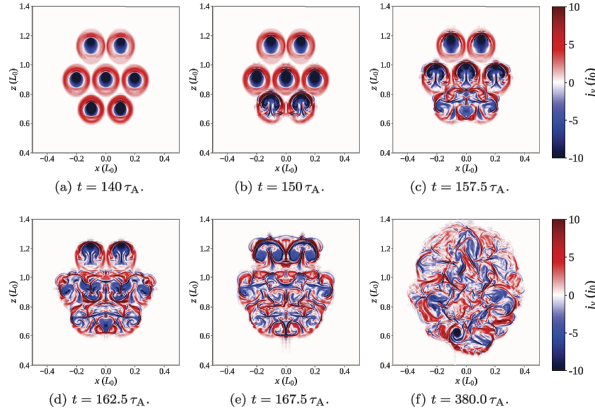


Figure 25. Contours of the toroidal currents in a cut above the polarity inversion line, for different times (see details in¹⁸¹) Reproduced with permission from Threlfal et al., *Solar Physics*, **296**, 120 (2021), Copyright 2021 Springer.

oped convective layer. The gradual emergence of the field into the solar atmosphere results in a network of magnetic loops, which interact dynamically, forming current layers at their interfaces. They find that these CoSs are short-lived (from 30 s to minutes), giving rise to bursts of energy in the range 10^{25} – 10^{27} erg, which basically is the microflare range. The CoSs' persistent formation, interaction, and evolution leads to recurrent emission of fast EUV/X-ray jets and to considerable plasma heating in the active corona.

All attempts to model the non linear coupling and the evolution of the emerged magnetic fields, driven by photospheric and subphotospheric motions, can be explored with one more tool. Non linear extrapolation of the force free magnetic field gives an approximate snapshot of the turbulent state in a coronal active region.

Kanella and Gudisken^{173,174,183} used a 3D MHD numerical code to simulate the region from the solar con-

vection zone up to the solar corona. The code includes different processes occurring in the convection zone, photosphere, chromosphere, transition region and corona. The simulated volume starts 2.5 Mm below the photosphere and extends 14.3 Mm above the photosphere into the corona. They used periodic boundary conditions in the horizontal $x\hat{y}$ -plane; in the vertical z -direction, the upper boundary is open, while the lower boundary is also open, but remains in hydrostatic equilibrium, enabling convective flows to enter and leave the system. They incorporated two strongly magnetic regions of opposite polarity, which are connected through a magnetic structure with a loop-like shape. The magnetic field is initially set vertically at the bottom boundary and extrapolated to the whole atmosphere, assuming a potential field, while a horizontal field of 100 Gauss is continuously fed in at the lower boundary, producing random bipolar structures in the photosphere. Identifying locations with 3D current sheets, as we have already discussed in section II, turns out not to be so simple. The CSs in 3D are generally not 2D flat structures, as the cartoon-like pictures of 2D reconnection would suggest, but they are much more complex. Often, the background current level is higher in places with many current sheets, so it is not easy to separate one current sheet from a cluster of CSs. This is in some ways similar to the problems experienced by observers, where the background is causing large obstacles for the interpretation. The method Kamela and Gudisken¹⁷³ have applied to identify CSs is called ImageJ, used in medical imaging and bio-informatics to perform multi-dimensional image analysis. Fig. 26(a) shows the 4136 identified CSs in the coronal part of the simulation volume, for a certain time-instant during the simulation. In Fig. 26(b), the differential size distribution of the identified CSs' released energy rate is plotted in logarithmic scales, which obey a power-law scaling with an index -1.5 .

Einaudi et al.⁴³ discussed the differences between "nanoflares", introduced by Parker, and "elementary events," defined in their article as small-scale spatially and temporally isolated heating events, resulting from the continuous formation and dissipation of field-aligned current sheets within a coronal loop. They presented numerical simulations of the compressible 3D MHD equations. They used two clustering algorithms to investigate the properties of the simulated elementary events: an IDL implementation of a density-based spatial clustering technique for applications with noise, and their own physical distance clustering algorithm. They identified and tracked elementary heating events in time, and for every event they characterized properties such as density, temperature, volume, aspect ratio, length, thickness, duration, and energy. The energies of the events are in the range of 10^{18} – 10^{21} erg, with durations shorter than 100 s. A few events last up to 200 s and release energies up to 10^{23} erg. While high temperatures are typically located at the flux tube apex, the currents extend all the way to the footpoints. Hence, a single elementary event

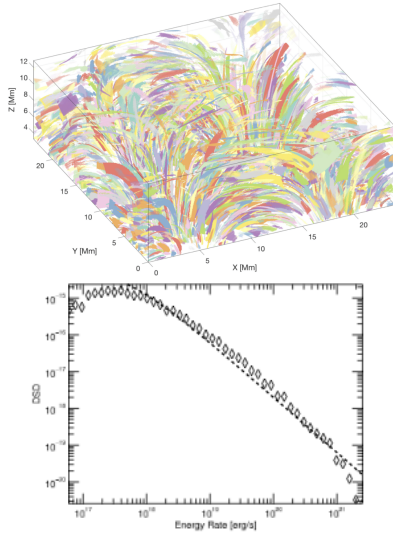


Figure 26. (a) 3D magnetic topology in the solar corona, with 4136 identified CSs; each color represents a different CS. (b) Differential size distribution of the identified CSs' energy rate in logarithmic scale (diamonds). A power law fit (dashed) yields the index $\sim -1.50 \pm 0.02$ (see Kanella and Gudisen¹⁷³ for details. Reproduced with permission from Kanella and Gudisen, *Astronomy and Astrophysics*, **603**, 83 (2017), Copyright 2021 ESO.

cannot be detected at present. The observed emission is due to the superposition of many elementary events, distributed randomly in space and time within a loop.

The formation of CSs and other CoSs in the solar atmosphere, driven by the turbulent convection zone, depends on the magnetic topology above the photosphere (e.g. single magnetic flux tube, multi-flux magnetic tubes, etc), and on the details of the convection zone driver (small scale stochastic motion, turbulent motions, emerging magnetic flux, etc). All articles listed above followed the initial conjecture of Parker¹⁵⁹ and focused on the formation of randomly distributed small scale CSs inside a volume, which subsequently will provide Ohmic heating in the Corona. It was assumed, without any proof, that the current sheets formed and the energy released are very small (“nanoflares” or “elementary events”, with energy in the range $\approx 10^{20} - 10^{21}$ erg). In our opinion, this assumption was not supported by the MHD simulations, since the flux tubes, or the multiple flux tubes, or the complex magnetic topologies are filled with CoSs at all scales. The observed explosive phenomena and flares in closed magnetic topologies are also present in the strongly turbulent solar corona and follow the statistical properties reported¹⁶⁴ when the turbulent corona is driven by turbulent photospheric motions. We must emphasize here that the magnetic coupling of the convection zone with the solar atmosphere and the formation of CoSs is a multi-scale process, ranging from 10^{11} cm to a few cm.

2. Formation of CoSs during explosive events associated with large scale reorganizations of the magnetic field in the solar atmosphere

A 3D study of solar explosions associated with CMEs is also a multiscale problem. Cheung et al.¹⁸⁴ used a 3D MHD code to capture the large scale of such explosions. Their simulation domain captured the top 7500 km of the solar convection zone, and the first 41600 km of the overlying solar atmosphere. The initial set up was inspired by the observed evolution of a specific Active Region (AR), but was not intended to model a specific flare of the specific AR. The initial setup consisted of a bipolar sunspot pair, each with a magnetic flux of 3.4×10^{21} Mx. A strongly twisted magnetic bipole with 10^{21} Mx flux emerged in proximity to one of the pre-existing sunspots. The emergence of the parasitic bipole leads to the creation of a twisted coronal flux rope well before the flare onset. The code of Cheung et al.¹⁸⁴ is ideal to capture the large scale evolution, but it misses all the physical processes related with the formation of CoSs and their interaction with particles. Therefore, two more levels of scales are necessary to be included in such an analysis. A hybrid code can capture the formation of CoSs (meso-scales), and a kinetic code can explore the details of the collective dissipation of CoSs and the heating and acceleration of particles.

Inoue et al.^{132,185} used a 3D MHD code to analyze a specific flare/eruption of a specific AR. Their starting point was the nonlinear force free field (NLFFF) extrapolation¹³¹ of the magnetogram. In Fig. 27, the large scale evolution of the eruption is shown. The striking part in this simulation is the presence of thousands of magnetic flux ropes (MFR), which are twisted and evolve, possibly interacting with each other. Based on the analysis presented in the previous subsection, an individual MFR⁴⁰ and a collection of MFRs¹⁸¹ can create a dense environment of CoSs along with the evolving MFRs and their interaction. As shown in Fig. 27, Inoue et al focused their analysis on the formation of the large scale CS in the middle of the huge structure. The fragmentation of this structure and the formation of smaller scale structures, as we reported earlier, was beyond the resolution of their simulation (see also He et al.¹⁸⁶).

The evolution of a large collection of MFRs was studied with the use of 3D MHD codes recently by several authors (see^{186,187} and references therein). Jiang et al.¹⁸⁷ used a fully 3D MHD simulation with high accuracy to follow solar eruptions. They initiated the simulation with a bipolar configuration with no additional special magnetic topology. The bipolar configuration was driven unstable by a photospheric shearing motion. Once the large-scale CoSs and CSs are formed and reconnection starts, the whole arcade expands explosively, forming fast expanding twisted flux ropes with very strong turbulence in the volume underneath (see Fig. 28). The simplicity and efficiency of their scenario highlights the importance of the magnetic topology driven unstable and the role of

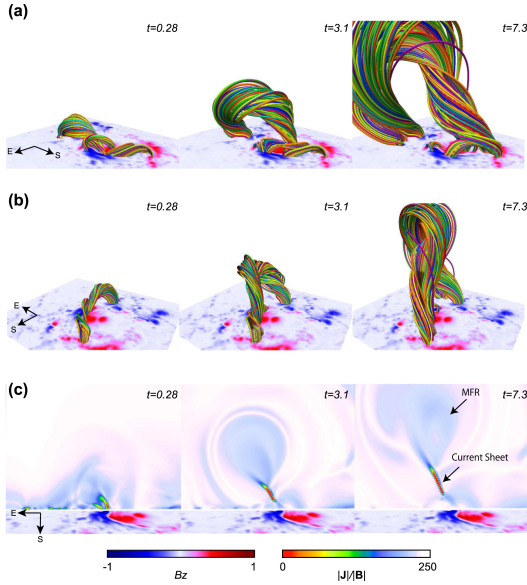


Figure 27. Temporal evolution of the formation and dynamics of the eruptive magnetic flux ropes (MFRs). Panels (a) and (b) show the field lines from different viewing angles. E and S stand for east and south. (c) Temporal evolution of $|J|/|B|$, plotted in the $x\hat{a}z$ -plane. Reproduced with permission from Inoue et al., *The Astrophysical Journal*, **867**, 83 (2018), Copyright 2018 AAS

the driver. After all, when using a realistic magnetic topology and a turbulent photospheric driver or emerging magnetic field, large scale CoSs very quickly fragment (see more on this in section III) and drive strong turbulence.

Several authors^{178,188}, analyzed the stressing of an isolated flux rope (FR) (which is part of the highly stressed large scale magnetic topologies shown in Figs. 27 and 28) at the two ends by large scale localized photospheric vortical motion, which twists the coronal field lines, and the resulting current fragmentation reaches again the state of strong turbulence, as discussed earlier.

As we mentioned already in Sect. 3, magnetic flux emergence and the subsequent eruptions, with the formation of jets, was studied in many articles^{117–126}. Most of the numerical studies stopped their analysis at the formation of a large scale current sheet through the interaction of the emerging flux tube with the ambient magnetic field of the solar atmosphere.

We can then conclude that during large scale magnetic explosions, the fragmentation of formed large scale CSs, and the formation of CoSs through the stresses resulting from eruptions inside MFRs reported above, are extremely important for the analysis of the heating and acceleration of the coronal plasma during eruptions and large scale reorganization of the magnetic field of an active region. The fact that solar flares and the associated CMEs were modeled so far as 2D structures with a monolithic large scale CS as the main source of the energy released (called by many researchers the **standard**

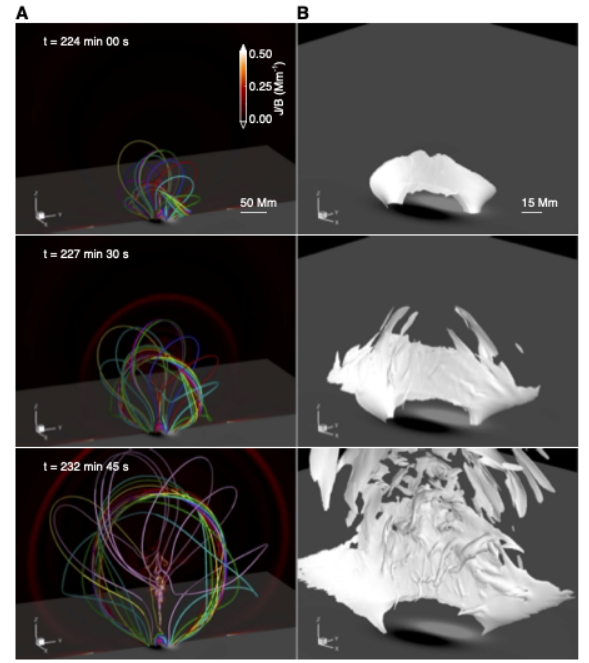


Figure 28. Evolution of magnetic field lines and the large scale CS in 3D during the eruption. (A) The magnetic field lines are shown by thick colored lines, where the colours are used for a better visualization of the different lines. Note that the MFR is weakly twisted in its core but highly twisted in its envelope. The bottom surface is shown with the distribution of the magnetic flux. The vertical, transparent slice shows the distribution of the current density normalized by the magnetic field strength, i.e. J/B . (B) The CS in the 3D configuration is shown as iso-surface for $J/B = 0.5 \text{ Mm}^{-1}$. Reproduced with permission from Jiang et al., *Physics of Fluids*, **33**, 055133 (2021), Copyright 2018 AIP

flare) has misled the analysis of the observed data resulting from the heating and acceleration of particles during solar explosions.

VI. FORMATION AND EVOLUTION OF COHERENT STRUCTURES AND SELF ORGANIZED CRITICALITY

We have repeatedly stated in this review that many space and astrophysical systems have a turbulent driver as a source of their strong turbulence, e.g. the convection zone acts as a driver for the magnetic field extending from the convection zone into the solar atmosphere and the solar wind, solar wind turbulence acts as the driver in the vicinity of the Earth's bow shock, the magnetosheath, and the magnetotail, etc. In the previous section, we focused our analysis on the magnetic coupling of the convection zone with the solar atmosphere (see Fig. 29), utilizing mainly 3D MHD codes to concentrate on the evolution of the driven system at the large scales¹⁸⁹.

In Fig. 29, we present a scenario to reconstruct the formation of CoSs in an active region, using a simple cartoon. The starting point is a 3D large scale magnetic

topology, which can be estimated by force-free extrapolation of the photospheric magnetic field. The more intense magnetic structures are forming active regions (ARs) (see Fig. 29a). As discussed extensively in Sec. V, the formation of CoSs inside an AR is shown in Fig. 29b. Only a small number of CoSs are forming CSs inside an AR, and from them an again small fraction will reconnect (see Fig. 29c, d). This is a multi scale system, extending from 100 - 1000 Mm in the initial box (Fig. 29(a)) down to a few cm's at the scale of the reconnecting CSs (Fig. 29d).

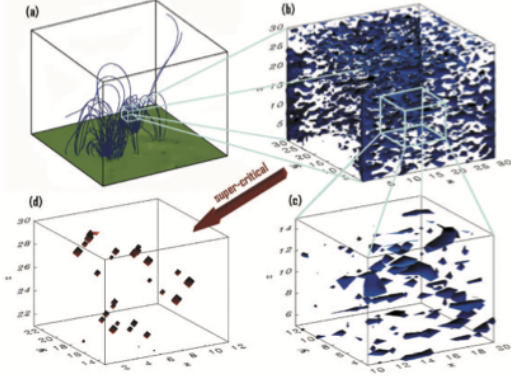


Figure 29. (a) Force-free magnetic field lines, extrapolated from the convection zone into the corona. (b) CoSs in a sub-volume of a coronal active region. (c) Same as (b), but zoomed. (d) Spatial distribution of the reconnecting CSs inside a sub-volume of the complex active region. Reproduced with permission from Vlahos et al., The Astrophysical Journal, **608**, 540 (2004), Copyright 2004 AAS

The existing numerical tools cannot handle the multi scale coupling of the convection zone with the solar atmosphere, so we are searching for other tools to explore the formation of CoSs in the solar atmosphere.

In this section, we will concentrate on numerical tools that are used extensively in the analysis of complex systems (e.g. systems far away from equilibrium, like strong turbulence, or systems comprised of a large number of nonlinearly interacting sub-systems, like a collection of CoSs in a turbulent plasma). The most popular numerical tool used to analyze complex systems is the Cellular Automaton (CA) model¹⁹⁰. The set up of the CA depends strongly on a qualitative analysis of the physical system under study, which guides the definition of the rules of the CA. The success of a CA model is assessed by the direct comparison with data and results from MHD simulations. So complex systems, like turbulent plasmas, can be explored by CA models (on the global astrophysical scales), and by MHD or kinetic simulations on the intermediate and the local scales. Also, MHD and kinetic simulations can serve as tools for defining the rules of a CA.

The existence of power laws in the frequency distributions of the explosive solar activity (see Fig. 20) may suggest that explosions are a self-organization phenomenon in ARs. Lu and Hamilton¹⁹¹ (LH91) were the

first to realize that ARs may be in a self-organized critical state, and they proposed that explosions ultimately are caused by small magnetic perturbations (δB) (**loading**), which gradually force a CS to reconnect when a **local critical threshold** is passed. The local fragmentation of the reconnecting CSs (see section III) causes a re-organization of the unstable magnetic topology, which may cause **avalanches** of CSs at all scales to reconnect and to release energy (nano-flares, micro-flares, flares) (the basic ideas of SOC were initially proposed by Bak et al.¹⁹², thirty five years ago). The LH91 model opened the way for a series of similar models developed during the last twenty five years (see the reviews by^{166,189,193,194}).

There are many ways to develop CA models to represent SOC¹⁹⁴, one of them based its rules on the MHD equations^{195,196}. The proposed set-up can be superimposed onto each classical solar flare CA model, making the latter interpretable in a MHD-consistent way (*classical* CA models here means the LH91 model¹⁹¹ and its modifications, which are based on the sand-pile analogy^{197–199}). The set-up thus specifies the physical interpretation of the grid-variables and allows the derivation of quantities such as currents etc. It does not interfere with the dynamics of the CA (unless wished): loading, redistributing (bursting), and the appearance of avalanches and Self-Organized Criticality (SOC), if the latter are implied by the evolution rules, remain unchanged. The result is therefore still a CA model, with all the advantages of CAs, namely that they are fast, that they model large spatial regions (and large events), and therewith that they yield good statistics. Since the set-up introduces all the relevant physical variables into the context of a CA model, it automatically leads to a better physical understanding of the CA models. It reveals which relevant plasma processes and in what form are actually implemented, and what the global flare scenario is the CA models imply. All this is more or less hidden otherwise in the abstract evolution rules. It leads also to the possibility to change the CA models (the rules) at the guide-line of MHD, if this should become desirable. Not least, the set-up opens a way for further comparison of the CA models to observations.

The specifications the set-up meets are: The vector \mathbf{A}_{ijk} at the grid sites \mathbf{x}_{ijk} denotes the local vector-field, $\mathbf{A}(\mathbf{x}_{ijk})$. Note that this was not specified in the classical CA models. Lu et al.²⁰⁰ for instance discussed this point: it might also have been thought of as a mean local field, i.e. the average over an elementary cell in the grid.

Guided by the idea that one wants to assure $\nabla \cdot \mathbf{B} = 0$ for the magnetic field \mathbf{B} , which is most easily achieved by having the vector-potential \mathbf{A} as the primary variable and letting \mathbf{B} be the corresponding derivative of \mathbf{A} ($\mathbf{B} = \nabla \times \mathbf{A}$), it is furthermore assumed that the grid variable \mathbf{A} of the CA model is identical with the vector-potential.

The remaining and actually most basic problem then is to find an adequate way to calculate derivatives in the grid. In general, CA models assume that the grid-spacing is finite, which also holds for the CA model of¹⁹¹ (as

shown in detail by²⁰¹), so that the most straightforward way of replacing differential expressions with difference expressions is not adequate. Consequently, one has to find a way of continuing the vector-field into the space in-between the grid-sites, which will allow to calculate derivatives. For this purpose, Isliker, Anastasiadis, and Vlahos^{195,196} proposed to use spline interpolation, where the 3D interpolation is performed as three subsequent 1D interpolations in the three spatial directions²⁰². For the 1D splines, natural boundaries are assumed (the second derivatives are zero at the boundaries).

With the help of this interpolation, the magnetic field \mathbf{B} and the current \mathbf{J} are calculated as derivatives of \mathbf{A} , according to the MHD prescription:

$$\mathbf{B} = \nabla \times \mathbf{A}, \quad (8)$$

$$\mathbf{J} = \frac{c}{4\pi} \nabla \times \mathbf{B}. \quad (9)$$

According to MHD, the electric field is given by Ohm's law, $\mathbf{E} = \eta \mathbf{J} - \frac{1}{c} \mathbf{v} \times \mathbf{B}$, with η the diffusivity and \mathbf{v} the fluid velocity. Since the classical CA models use no velocity-field, the set-up can yield only the resistive part,

$$\mathbf{E} = \eta \mathbf{J}. \quad (10)$$

In applications such as to solar explosions, where the interest is in current dissipation events, i.e. in events where η and \mathbf{J} are strongly increased, Eq. 10 can be expected to be a good approximation to the electric field. Theoretically, the convective term in Ohm's law would in general yield just a low-intensity, background electric field.

Eq. (10) needs to be supplemented with a specification of the diffusivity η : Isliker *et al.*²⁰¹ have shown that in the classical CA models the diffusivity adopts the values $\eta = 1$ at the unstable (bursting) sites, and $\eta = 0$ everywhere else. This specifies Eq. (10) completely. The set-up of Isliker *et al.*^{195,196} for classical solar flare CA models yields, among others, consistency with Maxwell's equations (e.g. divergence-free magnetic field), and availability of secondary variables such as currents and electric fields in accordance with MHD. The main aim in Isliker, Anastasiadis, and Vlahos^{195,196} with the introduced set-up was to demonstrate that the set-up truly extends the classical CA models and makes them richer in the sense that they contain much more physical information. The main features they revealed about the classical CA models, extended with their set-up, are:

- 1. Large-scale organization of the vector-potential and the magnetic field:** The field topology during SOC state is bound to characteristic large-scale structures which span the whole grid, very pronounced for the primary grid variable, the vector-potential, but also for the magnetic field. Bursts and flares are just slight disturbances propagating over the large-scale structures, which are always maintained, also in the largest events.
- 2. Increased current at unstable grid-sites:** Unstable sites are characterized by an enhanced current, which

is reduced after a burst has taken place, as a result of which the current at a grid-site in the neighbourhood may be increased.

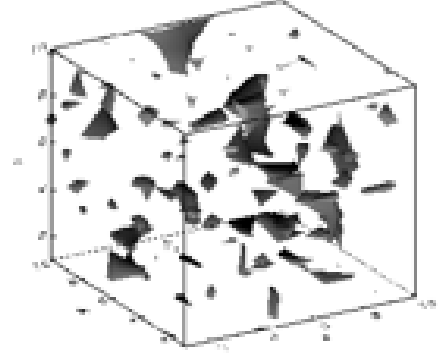


Figure 30. Three dimensional isosurfaces of the electric current density, as yielded by the CA model of Isliker, Anastasiadis, and Vlahos¹⁹⁵. Reproduced with permission from Isliker *et al.*, *Astronomy and Astrophysics*, **363**, 1068 (2000), Copyright 2000 ESO

3. Availability of the electric field: The electric field is calculated with the resistive part of Ohm's law, which can be expected to be a good approximation in applications where the interest is in current-dissipation events, e.g. in the case of solar flares.

4. Energy release in terms of Ohmic dissipation: Isliker, Anastasiadis, and Vlahos^{195,196} also replaced the somewhat *ad hoc formula* in the classical CA models to estimate the energy released in a burst with the expression for Ohmic dissipation in terms of the current. The distributions yielded in this way are very similar to the ones based on the *ad hoc formula*, so that the results of the CA models remain basically unchanged.

5. CA as models for current dissipations: As a consequence of point 2 and 4 in this list, and of the fact that there is an approximate linear relation between the current and the stress measure of the classical CAs, one can conclude that the *extended* CA models can be considered as models for energy release through current dissipation.

It is rather interesting to compare the 3D isosurfaces shown in Fig. 30 for the electric field generated by the CA model of Isliker, Anastasiadis, and Vlahos^{195,196} with the 3D MHD simulations reported in Galsgaard and Nordlund⁴⁰ and shown here in Fig. 21. It is remarkable to note the appearance of non-steady current surfaces in the MHD model, as it is the case in the CA model in Fig. 30.

Fragos *et al.*²⁰³ used “magnetograms” generated with the percolation method and applied a linear extrapolation to search for the statistical properties of the reconstructed coronal AR. Moraitis *et al.*²⁰⁴ did the same, using observational magnetograms, and they noticed that the re-organization of the magnetic fields is a potential way to identify reconnecting CSs in the coronal part of an AR. Dimitropoulou *et al.*^{205,206} used a series of observed magnetograms to drive the SOC model proposed by Is-

liker et al.^{195,196}. They obtained robust power laws in the distribution functions of the modeled flaring events, with scaling law indices that agree well with the observations.

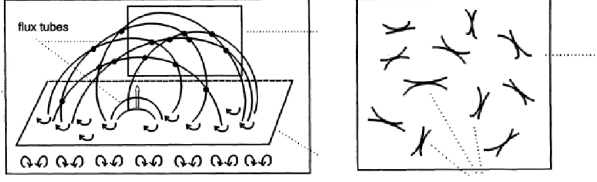


Figure 31. Formation of CSs developed intermittently at random positions. Reproduced with permission from Anastasiadis and Vlahos, *The Astrophysical Journal*, **428**, 819 (1994), Copyright 1994 AAS.

Models along these lines have been proposed^{207,208} (see also Fig. 31) in the mid 80's and the beginning of the 90's and remained undeveloped due to the lack of tools for the global analysis of active regions till recently. The nonlinear coupling of the turbulent convection zone with ARs, as well as the consistency of the related results obtained by the SOC theory with those from turbulence simulations, have been studied intensively by several authors²⁰⁹. Uritsky et al.²¹⁰ examined in depth the question of the relation of SOC with turbulence in the solar corona and agreed with the suggestion made by Dahlburg et al.²¹¹ that reconnecting CSs and their **fragmentation can serve as the driver for avalanches in the SOC scenario**. Uritsky & Devila²¹⁰ also suggested, by studying an AR in a quiescent non-flaring period, that (1) there is formation of non-potential magnetic structures with complex polarity separation lines inside the active region, and (2) there are statistical signatures of canceling bipolar magnetic structures coinciding with flaring activity in the active region. Each of these effects can give rise to an unstable magnetic configuration, acting as an energy source for coronal dissipation and heating. The development of a parallel use of models based on complexity theory and of well established 3D MHD or kinetic codes is the only way to explore the interplay between global and local scales in turbulent systems.

The tools used in this section focused on reconnecting CSs and cannot capture all types of CoSs in the driven turbulent system present in the solar atmosphere. Keeping track of CoSs that are not leading to reconnection, but still dissipate energy collectively in a large volume, is an open project for future models that will utilize tools of complexity theory.

VII. DISCUSSION AND SUMMARY

The formation of CoSs in 3D strongly turbulent magnetized plasma remains till today an open problem for the analysis of space, astrophysical and laboratory plasmas. The main obstacle remains the multi-scale characteristics, with the dynamic evolution taking place on

all scales. The list of intermittently appearing CoSs inside 3D strongly turbulent magnetized plasmas is long (CSs (non-reconnecting and reconnecting), magnetic filaments, large amplitude magnetic disturbances, vortices, shocklets, etc) and expanding. CSs and their reconnection are the best studied CoSs, but so far the vast majority of studies separated CSs and their evolution from the rest of the CoSs and the turbulent environment where they were formed. The other shortcoming in the analysis of CSs till today is the fact that their evolution was analyzed with analytical and numerical tools in 2D magnetic topologies. The other well known large scale magnetic discontinuities that were isolated from CoSs and a strongly turbulent environment in their vicinity are large scale shocks. Isolating CSs and shocks in their analysis from 3D magnetic topologies and the strongly turbulent environments, in which they are formed and evolve, can lead to an erroneous answer to the question “Who really needs turbulence?”.

In this review, we have addressed two important questions: (1) How CoSs are formed? We presented three different ways for the formation: (a) The formation of CoSs (with special emphasis on CSs) where 3D strong turbulence is present. Common space, astrophysical, and laboratory plasmas, where strong turbulence is present, are the solar atmosphere, the solar wind, astrophysical jets, edge localised mode turbulence in TOKAMAKS, etc. (b) The fragmentation of large scale CSs, appearing mostly in explosive phenomena in the solar atmosphere, in the magnetotail under the influence of the solar wind, and in the magnetopause under the influence of the magnetosheath. (c) The interaction of large scale shocks with strong turbulence upstream and downstream of the shock, as appearing in the interaction of the Earth's bow shock with the turbulent solar wind, at the termination shock in the heliosphere, and at super nova remnants. (2) How strong turbulence is excited in astrophysical settings and in laboratory plasmas. We have chosen in this review to address mainly the excitation of strong turbulence by the convection zone, by turbulent flows, and by the fragmentation of large scale CSs formed during coronal explosions and in the magnetotail.

Let us now summarize the main points in this review.

- CoSs are formed in strongly turbulent 3D magnetized plasmas.
- CSs formed inside a 3D strongly turbulent plasma cannot be analyzed as isolated 2D periodic structures.
- Only a small fraction of the CSs formed inside a 3D strongly turbulent plasma reconnect. Therefore, magnetic reconnection dominates the acceleration of the small fraction of high energy particles in the tail of the particles' energy distribution. The collective interaction of the non reconnecting CSs at all scales and with other CoSs (large scale magnetic disturbances, etc.) may play a crucial role in

the heating of the ambient plasma and the overall dissipation of energy.

- The methods developed so far to search in observed data for 3D CoSs in strongly turbulent plasmas are not sufficient to capture their statistical properties, since they have been based mainly on the 2D modeling of the characteristics of CoSs.
- The formation of large scale CSs and their subsequent fragmentation inside a turbulent plasma gives rise to clusters of CoSs in the vicinity of the CSs and contributes to the development of smaller scale activity inside the strongly turbulent system.
- Karimabadi et al.³⁷ and Grošelj et al.⁷⁴ emphasize that the motion of CoSs generates waves that are emitted into the ambient plasma in the form of highly oblique compressional and Alfvén modes, as well as large amplitude magnetic disturbances. This indicates that strong turbulence will in general consist of CoSs and waves, therefore "weak" and strong turbulence co-exist in the multiscale evolution of a strongly turbulent plasma.
- Large scale magnetic disturbances and CoSs in fully developed turbulence follow a mono-fractal or multi-fractal scaling, both in space and astrophysical plasmas. This strongly affects the interaction of particles with CoSs.
- Large scale shock waves, like CSs, never appear in isolation. They are formed in the presence of turbulent flows upstream and downstream. The presence of CoSs in the vicinity of a shock solves a number of open problems through the amplification of the CoSs near the shock discontinuity.
- Unfortunately, the multi-scale character and the complexity of the micro-physics present in evolving large scale shocks cannot be explored by current numerical simulations, and neither can they follow the evolution for long times. This is the main reason why we are missing many important details on the evolution of CoSs and their role in the heating and acceleration of particles so far.
- The magnetic coupling of the turbulent convection zone with the solar atmosphere has many avenues for forming CoSs and for exciting strong turbulence in the solar corona and the solar wind. We have emphasized two of them in this review, (1) magnetic foot-point shuffling of otherwise stable magnetic flux ropes, and magnetic field emerging into a complex magnetic topology, (2) explosive evolution of large scale magnetic structures (loss of equilibrium, triggered e.g. by emerging magnetic flux).
- The multi scale character of CoSs inside a strongly turbulent plasma cannot be addressed with the well known numerical tools (MHD codes, hybrid codes,

and particle in cell codes), since they capture only a part of the plasma evolution and cannot realize the self consistent coupling of all scales, and moreover they neglect the fact that most natural systems are open.

- The use of tools borrowed from complexity theory together with the 3D numerical codes mentioned above can be the solution for addressing the 3D nature of CoSs appearing inside a strongly turbulent plasma.

The statistical properties of 3D CoSs inside a strongly turbulent plasma are an interesting and important piece of information when analyzing the transport properties of charged particles in the complex topologies of CoSs. The energy dissipation of CoSs needs more careful analysis, and this problem is currently open and needs a separate review for its exposition.

ACKNOWLEDGMENTS

We would like to thank our colleagues Peter Cargill, Tassos Anastasiadis, Manolis Georgoulis, Vasilis Archontis, Rene Kluiving, Marco Onofri, Fabio Lepreti, Tasos Fragos, and Nikos Sioulas, for many interesting and constructive discussions over several years on the topics addressed in this review.

REFERENCES

- ¹U. Frisch, *Turbulence* (1996).
- ²D. Biskamp, *Magnetohydrodynamic Turbulence* (2003).
- ³W. H. Matthaeus, "Turbulence in space plasmas: Who needs it?" *Physics of Plasmas* **28**, 032306 (2021).
- ⁴A. A. Vedenov, "Quasi-linear plasma theory (theory of a weakly turbulent plasma)," *Journal of Nuclear Energy* **5**, 169–186 (1963).
- ⁵S. Galtier, "Wave turbulence in magnetized plasmas," *Nonlinear Processes in Geophysics* **16**, 83–98 (2009).
- ⁶P. Goldreich and S. Sridhar, "Toward a Theory of Interstellar Turbulence. II. Strong Alfvénic Turbulence," *Astrophys. J.* **438**, 763 (1995).
- ⁷J. C. Perez and S. Boldyrev, "On Weak and Strong Magnetohydrodynamic Turbulence," *Astrophysical Journal Letters* **672**, L61 (2008), arXiv:0712.2086 [astro-ph].
- ⁸L. Vlahos and H. Isliker, "Particle acceleration and heating in a turbulent solar corona," *Plasma Physics and Controlled Fusion* **61**, 014020 (2019), arXiv:1808.07136 [astro-ph.HE].
- ⁹M. Wan, W. H. Matthaeus, V. Roytershteyn, T. N. Parashar, P. Wu, and H. Karimabadi, "Intermittency, coherent structures and dissipation in plasma turbulence," *Physics of Plasmas* **23**, 042307 (2016).
- ¹⁰O. Pezzi, H. Liang, J. L. Juno, P. A. Cassak, C. L. Vásconez, L. Sorriso-Valvo, D. Perrone, S. Servidio, V. Roytershteyn, J. M. TenBarge, and W. H. Matthaeus, "Dissipation measures in weakly collisional plasmas," *Monthly Notices of the Royal Astronomical Society* **505**, 4857–4873 (2021), arXiv:2101.00722 [physics.plasm-ph].
- ¹¹H. Karimabadi and A. Lazarian, "Magnetic reconnection in the presence of externally driven and self-generated turbulence," *Physics of Plasmas* **20**, 112102 (2013).

- ¹²N. Sioulas, H. Isliker, and L. Vlahos, "Particle heating and acceleration by reconnecting and nonreconnecting current sheets," *Astronomy & Astrophysics* **657**, A8 (2022), arXiv:2107.08314 [astro-ph.SR].
- ¹³V. Carbone, P. Veltri, and A. Mangeney, "Coherent structure formation and magnetic field line reconnection in magnetohydrodynamic turbulence," *Physics of Fluids A* **2**, 1487–1496 (1990).
- ¹⁴B. T. Tsurutani and E. J. Smith, "Interplanetary discontinuities: Temporal variations and the radial gradient from 1 to 8.5 AU," *Journal of Geophysics Research* **84**, 2773–2787 (1979).
- ¹⁵M. Neugebauer, D. R. Clay, B. E. Goldstein, B. T. Tsurutani, and R. D. Zwickl, "A reexamination of rotational and tangential discontinuities in the solar wind," *Journal of Geophysics Research* **89**, 5395–5408 (1984).
- ¹⁶E. N. Parker, "Sweet's Mechanism for Merging Magnetic Fields in Conducting Fluids," *Journal of Geophysics Research* **62**, 509–520 (1957).
- ¹⁷H. E. Petschek, "Magnetic Field Annihilation," in *NASA Special Publication*, Vol. 50 (1964) p. 425.
- ¹⁸E. G. Zweibel and M. Yamada, "Perspectives on magnetic reconnection," *Proceedings of the Royal Society of London Series A* **472**, 20160479 (2016).
- ¹⁹N. F. Loureiro and D. A. Uzdensky, "Magnetic reconnection: from the Sweet-Parker model to stochastic plasmoid chains," *Plasma Physics and Controlled Fusion* **58**, 014021 (2016), arXiv:1507.07756 [physics.plasm-ph].
- ²⁰M. Hesse and P. A. Cassak, "Magnetic Reconnection in the Space Sciences: Past, Present, and Future," *Journal of Geophysical Research (Space Physics)* **125**, e25935 (2020).
- ²¹A. Lazarian and E. T. Vishniac, "Reconnection in a Weakly Stochastic Field," *Astrophys. J.* **517**, 700–718 (1999), astro-ph/9811037.
- ²²G. Kowal, A. Lazarian, E. T. Vishniac, and K. Otmianowska-Mazur, "Numerical Tests of Fast Reconnection in Weakly Stochastic Magnetic Fields," *Astrophysical Journal* **700**, 63–85 (2009), arXiv:0903.2052 [astro-ph.GA].
- ²³E. T. Vishniac, S. Pillsworth, G. Eyink, G. Kowal, A. Lazarian, and S. Murray, "Reconnection current sheet structure in a turbulent medium," *Nonlinear Processes in Geophysics* **19**, 605–610 (2012).
- ²⁴G. Kowal, A. Lazarian, E. T. Vishniac, and K. Otmianowska-Mazur, "Reconnection studies under different types of turbulence driving," *Nonlinear Processes in Geophysics* **19**, 297–314 (2012), arXiv:1203.2971 [astro-ph.SR].
- ²⁵L. Comisso, D. Grasso, and F. L. Waelbroeck, "Extended theory of the Taylor problem in the plasmoid-unstable regime," *Physics of Plasmas* **22**, 042109 (2015), arXiv:1502.06408 [physics.plasm-ph].
- ²⁶B. Coppi, G. Laval, and R. Pellat, "Dynamics of the Geomagnetic Tail," *Physical Review Letters* **16**, 1207–1210 (1966).
- ²⁷W. H. Matthaeus and S. L. Lamkin, "Turbulent magnetic reconnection," *Physics of Fluids* **29**, 2513–2534 (1986).
- ²⁸J. F. Drake, M. Swisdak, H. Che, and M. A. Shay, "Electron acceleration from contracting magnetic islands during reconnection," *Nature* **443**, 553–556 (2006).
- ²⁹M. Hoshino and Y. Lyubarsky, "Relativistic Reconnection and Particle Acceleration," *Space Science Reviews* **173**, 521–533 (2012).
- ³⁰S. Adhikari, M. A. Shay, T. N. Parashar, P. S. Pyakurel, W. H. Matthaeus, D. Godzieba, J. E. Stawarz, J. P. Eastwood, and J. T. Dahlin, "Reconnection from a turbulence perspective," *Physics of Plasmas* **27**, 042305 (2020), arXiv:1911.06219 [physics.plasm-ph].
- ³¹S. Servidio, W. H. Matthaeus, M. A. Shay, P. A. Cassak, and P. Dmitruk, "Magnetic Reconnection in Two-Dimensional Magnetohydrodynamic Turbulence," *Physical Review Letters* **102**, 115003 (2009).
- ³²P. D. Mininni, A. Alexakis, and A. Pouquet, "Energy transfer in Hall-MHD turbulence: cascades, backscatter, and dynamo action," *Journal of Plasma Physics* **73**, 377–401 (2007), arXiv:physics/0510053 [physics.plasm-ph].
- ³³D. Biskamp and H. Welter, "Dynamics of decaying two-dimensional magnetohydrodynamic turbulence," *Physics of Fluids B* **1**, 1964–1979 (1989).
- ³⁴W. H. Matthaeus and M. Velli, "Who Needs Turbulence?. A Review of Turbulence Effects in the Heliosphere and on the Fundamental Process of Reconnection," *Space Science Reviews* **160**, 145–168 (2011).
- ³⁵P. Cargill, L. Vlahos, G. Baumann, J. Drake, and Å. Nordlund, "Current fragmentation and particle acceleration in solar flares," *Space science reviews* **173**, 223–245 (2012).
- ³⁶A. Lazarian, L. Vlahos, G. Kowal, H. Yan, A. Beresnyak, and E. d. G. Dal Pino, "Turbulence, magnetic reconnection in turbulent fluids and energetic particle acceleration," *Space science reviews* **173**, 557–622 (2012).
- ³⁷H. Karimabadi, V. Roytershteyn, H. X. Vu, Y. A. Omelchenko, J. Scudder, W. Daughton, A. Dimmock, K. Nykyri, M. Wan, D. Sibeck, M. Tatineni, A. Majumdar, B. Loring, and B. Geveci, "The link between shocks, turbulence, and magnetic reconnection in collisionless plasmas," *Physics of Plasmas* **21**, 062308 (2014).
- ³⁸E. N. Parker, "Magnetic neutral sheets in evolving fields. I - General theory," *Astrophys. J.* **264**, 635–647 (1983).
- ³⁹E. N. Parker, "Nanoflares and the solar X-ray corona," *Astrophys. J.* **330**, 474–479 (1988).
- ⁴⁰K. Galsgaard and Å. Nordlund, "Heating and activity of the solar corona 1. Boundary shearing of an initially homogeneous magnetic field," *Journal Geoph. Res* **101**, 13445–13460 (1996).
- ⁴¹K. Galsgaard and Å. Nordlund, "Heating and activity of the solar corona. 2. Kink instability in a flux tube," *Journal Geoph. Res.* **102**, 219–230 (1997).
- ⁴²K. Galsgaard and Å. Nordlund, "Heating and activity of the solar corona. 3. Dynamics of a low beta plasma with three-dimensional null points," *Journal Geoph. Res.* **102**, 231–248 (1997).
- ⁴³G. Einaudi, R. B. Dahlburg, I. Ugarte-Urra, J. W. Reep, A. F. Rappazzo, and M. Velli, "Energetics and 3D Structure of Elementary Events in Solar Coronal Heating," *Astrophysical Journal* **910**, 84 (2021), arXiv:2103.13499 [astro-ph.SR].
- ⁴⁴P. Dmitruk, W. Matthaeus, N. Seenu, and M. R. Brown, "Test particle acceleration in three-dimensional magnetohydrodynamic turbulence," *Astrophys. J. Lett.* **597**, L81 (2003).
- ⁴⁵K. Arzner, B. Knaepen, D. Carati, N. Denewet, and L. Vlahos, "The Effect of Coherent Structures on Stochastic Acceleration in MHD Turbulence," *Astrophys. J.* **637**, 322–332 (2006), astro-ph/0509717.
- ⁴⁶S. Servidio, W. H. Matthaeus, M. A. Shay, P. Dmitruk, P. A. Cassak, and M. Wan, "Statistics of magnetic reconnection in two-dimensional magnetohydrodynamic turbulence," *Physics of Plasmas* **17**, 032315 (2010).
- ⁴⁷S. Servidio, P. Dmitruk, A. Greco, M. Wan, S. Donato, P. A. Cassak, M. A. Shay, V. Carbone, and W. H. Matthaeus, "Magnetic reconnection as an element of turbulence," *Nonlinear Processes in Geophysics* **18**, 675–695 (2011).
- ⁴⁸V. Zhdankin, D. A. Uzdensky, J. C. Perez, and S. Boldyrev, "Statistical Analysis of Current Sheets in Three-dimensional Magnetohydrodynamic Turbulence," *Astrophys. J.* **771**, 124 (2013), arXiv:1302.1460 [astro-ph.HE].
- ⁴⁹F. Valentini, S. Servidio, D. Perrone, F. Califano, W. H. Matthaeus, and P. Veltri, "Hybrid Vlasov-Maxwell simulations of two-dimensional turbulence in plasmas," *Physics of Plasmas* **21**, 082307 (2014).
- ⁵⁰S. S. Cerri and F. Califano, "Reconnection and small-scale fields in 2D-3V hybrid-kinetic driven turbulence simulations," *New Journal of Physics* **19**, 025007 (2017).
- ⁵¹H. Isliker, L. Vlahos, and D. Constantinescu, "Fractional Transport in Strongly Turbulent Plasmas," *Physical Review Letters* **119**, 045101 (2017), arXiv:1707.01526 [physics.plasm-ph].
- ⁵²L. Comisso and L. Sironi, "The Interplay of Magnetically Dom-

- inated Turbulence and Magnetic Reconnection in Producing Nonthermal Particles,” *Astrophysical Journal* **886**, 122 (2019), [arXiv:1909.01420 \[astro-ph.HE\]](#).
- ⁵³J. A. Agudelo Rueda, D. Verscharen, R. T. Wicks, C. J. Owen, G. Nicolaou, A. P. Walsh, I. Zouganelis, K. Germaschewski, and S. Vargas Domínguez, “Three-dimensional magnetic reconnection in particle-in-cell simulations of anisotropic plasma turbulence,” *Journal of Plasma Physics* **87**, 905870228 (2021), [arXiv:2103.13232 \[physics.space-ph\]](#).
- ⁵⁴P. Dmitruk, W. H. Matthaeus, and N. Seenu, “Test Particle Energization by Current Sheets and Nonuniform Fields in Magnetohydrodynamic Turbulence,” *Astrophys. J.* **617**, 667–679 (2004).
- ⁵⁵K. Arzner and L. Vlahos, “Particle acceleration in multiple dissipation regions,” *Astrophys. J. Lett.* **605**, L69 (2004).
- ⁵⁶J. P. Boyd, *Chebyshev and Fourier spectral methods* (Courier Corporation, 2001).
- ⁵⁷S. Gottlieb and C. W. Shu, “Total variation diminishing Runge-Kutta schemes,” *Mathematics of Computation* **67**, 73–85 (1998).
- ⁵⁸A. Greco, W. H. Matthaeus, S. Servidio, P. Chuychai, and P. Dmitruk, “Statistical Analysis of Discontinuities in Solar Wind ACE Data and Comparison with Intermittent MHD Turbulence,” *Astrophysical Journal Letters* **691**, L111–L114 (2009).
- ⁵⁹V. M. Uritsky, A. Pouquet, D. Rosenberg, P. D. Mininni, and E. F. Donovan, “Structures in magnetohydrodynamic turbulence: Detection and scaling,” *Phys. Rev. E* **82**, 056326 (2010), [arXiv:1007.0433 \[physics.flu-dyn\]](#).
- ⁶⁰C. Rossi, F. Califano, A. Retinò, L. Sorriso-Valvo, P. Henri, S. Servidio, F. Valentini, A. Chasapis, and L. Rezeau, “Two-fluid numerical simulations of turbulence inside Kelvin-Helmholtz vortices: Intermittency and reconnecting current sheets,” *Physics of Plasmas* **22**, 122303 (2015).
- ⁶¹E. De Giorgio, S. Servidio, and P. Veltri, “Coherent Structure Formation through nonlinear interactions in 2D Magnetohydrodynamic Turbulence,” *Scientific Reports* **7**, 13849 (2017).
- ⁶²S. Fadanelli, B. Lavraud, F. Califano, C. Jacquey, Y. Vernisse, I. Kacem, E. Penou, D. J. Gershman, J. Dorelli, C. Pollock, B. L. Giles, L. A. Avanov, J. Burch, M. O. Chandler, V. N. Coffey, J. P. Eastwood, R. Ergun, C. J. Farrugia, S. A. Fuselier, V. N. Genot, E. Grigorenko, H. Hasegawa, Y. Khotyaintsev, O. Le Contel, A. Marchaudon, T. E. Moore, R. Nakamura, W. R. Paterson, T. Phan, A. C. Rager, C. T. Russell, Y. Saito, J. A. Sauvaud, C. Schiff, S. E. Smith, S. Toledo Redondo, R. B. Torbert, S. Wang, and S. Yokota, “Four-Spacecraft Measurements of the Shape and Dimensionality of Magnetic Structures in the Near-Earth Plasma Environment,” *Journal of Geophysical Research (Space Physics)* **124**, 6850–6868 (2019).
- ⁶³D. Perrone, R. Bruno, R. D’Amicis, D. Telloni, R. De Marco, M. Stangalini, S. Perri, O. Pezzi, O. Alexandrova, and S. D. Bale, “Coherent Events at Ion Scales in the Inner Heliosphere: Parker Solar Probe Observations during the First Encounter,” *Astrophysical Journal* **905**, 142 (2020), [arXiv:2010.02578 \[astro-ph.SR\]](#).
- ⁶⁴M. Sisti, S. Fadanelli, S. S. Cerri, M. Faganello, F. Califano, and O. Agullo, “Characterizing current structures in 3D hybrid-kinetic simulations of plasma turbulence,” *Astronomy and Astrophysics* **655**, A107 (2021), [arXiv:2107.14130 \[physics.plasm-ph\]](#).
- ⁶⁵N. Sioulas, M. Velli, R. Chhiber, L. Vlahos, W. H. Matthaeus, R. Bandyopadhyay, M. E. Cuesta, C. Shi, T. A. Bowen, R. A. Qudsi, M. L. Stevens, and S. D. Bale, “Statistical analysis of intermittency and its association with proton heating in the near Sun environment,” *arXiv e-prints*, [arXiv:2201.10067 \(2022\)](#), [arXiv:2201.10067 \[astro-ph.SR\]](#).
- ⁶⁶C. Dong, L. Wang, Y.-M. Huang, L. Comisso, T. A. Sandstrom, and A. Bhattacharjee, “Reconnection-driven energy cascade in magnetohydrodynamic turbulence,” *Science Advances* **8**, eabn7627 (2022), [arXiv:2210.10736 \[astro-ph.SR\]](#).
- ⁶⁷L. Comisso and L. Sironi, “Ion and Electron Acceleration in Fully Kinetic Plasma Turbulence,” *Astrophysical Journal Letters* **936**, L27 (2022), [arXiv:2209.04475 \[astro-ph.HE\]](#).
- ⁶⁸T. Hada, D. Koga, and E. Yamamoto, “Phase coherence of MHD waves in the solar wind,” *Space Science Reviews* **107**, 463–466 (2003).
- ⁶⁹R. Bruno, B. Bavassano, L. Bianchini, E. Pietropaolo, U. Villante, V. Carbone, and P. Veltri, “Solar Wind Intermittency Studied via Local Intermittency Measure,” in *Magnetic Fields and Solar Processes*, ESA Special Publication, Vol. 9, edited by A. Wilson and et al. (1999) p. 1147.
- ⁷⁰A. Chasapis, Y. Yang, W. H. Matthaeus, T. N. Parashar, C. C. Haggerty, J. L. Burch, T. E. Moore, C. J. Pollock, J. Dorelli, D. J. Gershman, R. B. Torbert, and C. T. Russell, “Energy Conversion and Collisionless Plasma Dissipation Channels in the Turbulent Magnetosheath Observed by the Magnetospheric Multiscale Mission,” *Astrophysical Journal* **862**, 32 (2018).
- ⁷¹R. Chhiber, M. L. Goldstein, B. A. Maruca, A. Chasapis, W. H. Matthaeus, D. Ruffolo, R. Bandyopadhyay, T. N. Parashar, R. Qudsi, T. D. de Wit, S. D. Bale, J. W. Bonnell, K. Goetz, P. R. Harvey, R. J. MacDowall, D. Malaspina, M. Pulupa, J. C. Kasper, K. E. Korreck, A. W. Case, M. Stevens, P. Whittlesey, D. Larson, R. Livi, M. Velli, and N. Raouafi, “Clustering of Intermittent Magnetic and Flow Structures near Parker Solar Probe’s First Perihelion—A Partial-variance-of-increments Analysis,” *Astrophysical Journal Supplement* **246**, 31 (2020), [arXiv:1912.03608 \[physics.space-ph\]](#).
- ⁷²A. Greco, W. H. Matthaeus, S. Perri, K. T. Osman, S. Servidio, M. Wan, and P. Dmitruk, “Partial Variance of Increments Method in Solar Wind Observations and Plasma Simulations,” *Space Science Reviews* **214**, 1 (2018).
- ⁷³C. Jiang, R. Vinuesa, R. Chen, J. Mi, S. Laima, and H. Li, “An interpretable framework of data-driven turbulence modeling using deep neural networks,” *Physics of Fluids* **33**, 055133 (2021).
- ⁷⁴D. Grošelj, C. H. K. Chen, A. Mallet, R. Samtaney, K. Schneider, and F. Jenko, “Kinetic Turbulence in Astrophysical Plasmas: Waves and/or Structures?” *Physical Review X* **9**, 031037 (2019), [arXiv:1806.05741 \[physics.plasm-ph\]](#).
- ⁷⁵C. Y. Tu and E. Marsch, “Magnetohydrodynamic Structures Waves and Turbulence in the Solar Wind - Observations and Theories,” *Space Science Reviews* **73**, 1–210 (1995).
- ⁷⁶B. K. Shivamoggi, “Multi-Fractal Aspects of Spatial Intermittency in Fully Developed Magnetohydrodynamic Turbulence,” *Annals of Physics* **253**, 239–264 (1997).
- ⁷⁷D. Biskamp and W.-C. Müller, “Scaling properties of three-dimensional isotropic magnetohydrodynamic turbulence,” *Physics of Plasmas* **7**, 4889–4900 (2000).
- ⁷⁸E. Leonardis, S. C. Chapman, W. Daughton, V. Roytershteyn, and H. Karimabadi, “Identification of Intermittent Multifractal Turbulence in Fully Kinetic Simulations of Magnetic Reconnection,” *Physical Review Letters* **110**, 205002 (2013), [arXiv:1302.1749 \[physics.plasm-ph\]](#).
- ⁷⁹D. A. Schaffner and M. R. Brown, “Multifractal and Monofractal Scaling in a Laboratory MHD Turbulence Experiment,” *Astrophysical Journal* **811**, 61 (2015).
- ⁸⁰H. Isliker, V. Archontis, and L. Vlahos, “Particle Acceleration and Heating in Regions of Magnetic Flux Emergence,” *The Astrophysical Journal* **882**, 57 (2019).
- ⁸¹N. Sioulas, H. Isliker, and L. Vlahos, “Stochastic Turbulent Acceleration in a Fractal Environment,” *Astrophysical Journal Letters* **895**, L14 (2020), [arXiv:2005.02668 \[astro-ph.HE\]](#).
- ⁸²H. Karimabadi, V. Roytershteyn, M. Wan, W. H. Matthaeus, W. Daughton, P. Wu, M. Shay, B. Loring, J. Borovsky, E. Leonardis, S. C. Chapman, and T. K. M. Nakamura, “Coherent structures, intermittent turbulence, and dissipation in high-temperature plasmas,” *Physics of Plasmas* **20**, 012303 (2013).
- ⁸³A. Greco, F. Valentini, S. Servidio, and W. H. Matthaeus, “Inhomogeneous kinetic effects related to intermittent magnetic discontinuities,” *Physical Review E* **86**, 066405 (2012).
- ⁸⁴S. Servidio, K. T. Osman, F. Valentini, D. Perrone, F. Cali-

- fano, S. Chapman, W. H. Matthaeus, and P. Veltri, "Proton Kinetic Effects in Vlasov and Solar Wind Turbulence," *Astrophysical Journal Letters* **781**, L27 (2014), [arXiv:1306.6455 \[physics.space-ph\]](#).
- ⁸⁵E. Martinez, M. Hron, and J. Stöckel, "Coherent structures in the edge turbulence of the CASTOR tokamak," *Plasma Physics and Controlled Fusion* **44**, 351–359 (2002).
- ⁸⁶D. Galassi, P. Tamain, H. Bufferand, G. Ciraolo, P. Ghendrih, C. Baudoin, C. Colin, N. Fedorczak, N. Nace, and E. Serre, "Drive of parallel flows by turbulence and large-scale $E \times B$ transverse transport in divertor geometry," *Nuclear Fusion* **57**, 036029 (2017).
- ⁸⁷D. Galassi, G. Ciraolo, P. Tamain, H. Bufferand, P. Ghendrih, N. Nace, and E. Serre, "Tokamak edge plasma turbulence interaction with magnetic x-point in 3d global simulations," *Fluids* **4** (2019), [10.3390/fluids4010050](#).
- ⁸⁸X. Garbet, P. Mantica, F. Ryter, G. Cordey, F. Imbeaux, C. Sozzi, A. Manini, E. Asp, V. Parail, R. Wolf, and the JET EFDA Contributors, "Profile stiffness and global confinement," *Plasma Physics and Controlled Fusion* **46**, 1351–1373 (2004).
- ⁸⁹F. Wagner, G. Becker, K. Behringer, D. Campbell, A. Eberhagen, W. Engelhardt, G. Fussmann, O. Gehre, J. Gernhardt, G. v. Gierke, G. Haas, M. Huang, F. Karger, M. Keilhacker, O. Klüber, M. Kornherr, K. Lackner, G. Lisitano, G. G. Lister, H. M. Mayer, D. Meisel, E. R. Müller, H. Murmann, H. Niedermeyer, W. Poschenrieder, H. Rapp, H. Röhr, F. Schneider, G. Siller, E. Speth, A. Stäbler, K. H. Steuer, G. Venus, O. Vollmer, and Z. Yü, "Regime of improved confinement and high beta in neutral-beam-heated divertor discharges of the asdex tokamak," *Phys. Rev. Lett.* **49**, 1408–1412 (1982).
- ⁹⁰K. H. Burrell, "Effects of exb velocity shear and magnetic shear on turbulence and transport in magnetic confinement devices," *Physics of Plasmas* **4**, 1499–1518 (1997).
- ⁹¹H. Zohm, "REVIEW ARTICLE: Edge localized modes (ELMs)," *Plasma Physics and Controlled Fusion* **38**, 105–128 (1996).
- ⁹²J. W. Connor, "Edge-localized modes - physics and theory," *Plasma Physics and Controlled Fusion* **40**, 531–542 (1998).
- ⁹³A. W. Leonard, "Edge-localized-modes in tokamaks," *Physics of Plasmas* **21**, 090501 (2014).
- ⁹⁴C. Ham, A. Kirk, S. Pamela, and H. Wilson, "Filamentary plasma eruptions and their control on the route to fusion energy," *Nature Reviews Physics* **2**, 159–167 (2020).
- ⁹⁵V. Fundamenski, V. Naulin, T. Neukirch, O. E. Garcia, and J. J. Rasmussen, "On the relationship between ELM filaments and solar flares," *Plasma Physics and Controlled Fusion* **49**, R43–R86 (2007).
- ⁹⁶K. McClements, "Reconnection and fast particle production in tokamak and solar plasmas," *Advances in Space Research* **63**, 1443–1452 (2019).
- ⁹⁷H. Isliker, A. Cathey, M. Hoelzl, S. Pamela, and L. Vlahos, "Filamentary plasma eruptions and the heating and acceleration of electrons," *Physics of Plasmas* **29**, 112306 (2022).
- ⁹⁸W. H. Matthaeus, M. Wan, S. Servidio, A. Greco, K. T. Osman, S. Oughton, and P. Dmitruk, "Intermittency, nonlinear dynamics and dissipation in the solar wind and astrophysical plasmas," *Philosophical Transactions of the Royal Society of London A: Mathematical, Physical and Engineering Sciences* **373** (2015), [10.1098/rsta.2014.0154](#).
- ⁹⁹E. Yordanova, Z. Vörös, A. Varsani, D. B. Graham, C. Norgren, Y. V. Khotyaintsev, A. Vaivads, E. Eriksson, R. Nakamura, P. A. Lindqvist, G. Marklund, R. E. Ergun, W. Magnes, W. Baumjohann, D. Fischer, F. Plaschke, Y. Narita, C. T. Russell, R. J. Strangeway, O. Le Contel, C. Pollock, R. B. Torbert, B. J. Giles, J. L. Burch, L. A. Avanov, J. C. Dorelli, D. J. Gershman, W. R. Paterson, B. Lavraud, and Y. Saito, "Electron scale structures and magnetic reconnection signatures in the turbulent magnetosheath," *Journal of Geophysical Research* **43**, 5969–5978 (2016), [arXiv:1706.04053 \[physics.space-ph\]](#).
- ¹⁰⁰Z. Vörös, E. Yordanova, A. Varsani, K. J. Genestreti, Y. V. Khotyaintsev, W. Li, D. B. Graham, C. Norgren, R. Nakamura, Y. Narita, F. Plaschke, W. Magnes, W. Baumjohann, D. Fischer, A. Vaivads, E. Eriksson, P. A. Lindqvist, G. Marklund, R. E. Ergun, M. Leitner, M. P. Leubner, R. J. Strangeway, O. Le Contel, C. Pollock, B. J. Giles, R. B. Torbert, J. L. Burch, L. A. Avanov, J. C. Dorelli, D. J. Gershman, W. R. Paterson, B. Lavraud, and Y. Saito, "MMS Observation of Magnetic Reconnection in the Turbulent Magnetosheath," *Journal of Geophysical Research (Space Physics)* **122**, 11,442–11,467 (2017).
- ¹⁰¹K. Manolakou, A. Anastasiadis, and L. Vlahos, "Particle acceleration and radiation in the turbulent flow of a jet," *Astronomy and Astrophysics* **345**, 653–662 (1999).
- ¹⁰²C. Meringolo, A. Cruz-Orsorio, L. Rezzolla, and S. Servidio, "Microphysical Plasma Relations from Special-relativistic Turbulence," *Astrophys. J.* **944**, 122 (2023), [arXiv:2301.02669 \[astro-ph.HE\]](#).
- ¹⁰³L. Comisso, M. Lingam, Y. M. Huang, and A. Bhattacharjee, "General theory of the plasmoid instability," *Physics of Plasmas* **23**, 100702 (2016), [arXiv:1608.04692 \[physics.plasm-ph\]](#).
- ¹⁰⁴L. Comisso, M. Lingam, Y. M. Huang, and A. Bhattacharjee, "Plasmoid Instability in Forming Current Sheets," *Astrophys. J.* **850**, 142 (2017), [arXiv:1707.01862 \[astro-ph.HE\]](#).
- ¹⁰⁵A. Lazarian, G. L. Eyink, A. Jafari, G. Kowal, H. Li, S. Xu, and E. T. Vishniac, "3D turbulent reconnection: Theory, tests, and astrophysical implications," *Physics of Plasmas* **27**, 012305 (2020), [arXiv:2001.00868 \[astro-ph.HE\]](#).
- ¹⁰⁶M. Onofri, L. Primavera, F. Malara, and P. Veltri, "Three-dimensional simulations of magnetic reconnection in slab geometry," *Physics of Plasmas* **11**, 4837–4846 (2004).
- ¹⁰⁷M. Onofri, H. Isliker, and L. Vlahos, "Stochastic Acceleration in Turbulent Electric Fields Generated by 3D Reconnection," *Physical Review Letters* **96**, 151102 (2006), [astro-ph/0604192](#).
- ¹⁰⁸G. Kowal, E. M. de Gouveia Dal Pino, and A. Lazarian, "Magnetohydrodynamic Simulations of Reconnection and Particle Acceleration: Three-dimensional Effects," *Astrophysical Journal* **735**, 102 (2011), [arXiv:1103.2984 \[astro-ph.HE\]](#).
- ¹⁰⁹W. Daughton, V. Roytershteyn, H. Karimabadi, L. Yin, B. J. Albright, B. Bergen, and K. J. Bowers, "Role of electron physics in the development of turbulent magnetic reconnection in collisionless plasmas," *Nature Physics* **7**, 539–542 (2011).
- ¹¹⁰H. Karimabadi, V. Roytershteyn, W. Daughton, and Y.-H. Liu, "Recent evolution in the theory of magnetic reconnection and its connection with turbulence," *Space Science Reviews* **178**, 307–323 (2013).
- ¹¹¹J. S. Oishi, M.-M. Mac Low, D. C. Collins, and M. Tamura, "Self-generated Turbulence in Magnetic Reconnection," *Astrophysical Journal Letters* **806**, L12 (2015), [arXiv:1505.04653 \[astro-ph.SR\]](#).
- ¹¹²J. T. Dahlin, J. F. Drake, and M. Swisdak, "Electron acceleration in three-dimensional magnetic reconnection with a guide field," *Physics of Plasmas* **22**, 100704 (2015), [arXiv:1503.02218 \[physics.plasm-ph\]](#).
- ¹¹³G. Kowal, D. A. Falceta-Gonçalves, A. Lazarian, and E. T. Vishniac, "Statistics of Reconnection-driven Turbulence," *Astrophysical Journal* **838**, 91 (2017), [arXiv:1611.03914](#).
- ¹¹⁴D. Burgess, P. W. Gingell, and L. Matteini, "Multiple Current Sheet Systems in the Outer Heliosphere: Energy Release and Turbulence," *Astrophys. J.* **822**, 38 (2016), [arXiv:1603.06778 \[physics.space-ph\]](#).
- ¹¹⁵A. Greco, S. Perri, S. Servidio, E. Yordanova, and P. Veltri, "The Complex Structure of Magnetic Field Discontinuities in the Turbulent Solar Wind," *Astrophysical Journal Letters* **823**, L39 (2016), [arXiv:1511.03084 \[astro-ph.SR\]](#).
- ¹¹⁶R. Beg, A. J. B. Russell, and G. Hornig, "Evolution, Structure, and Topology of Self-generated Turbulent Reconnection Layers," *Astrophys. J.* **940**, 94 (2022), [arXiv:2209.04492 \[astro-ph.SR\]](#).
- ¹¹⁷J. Heyvaerts, E. R. Priest, and D. M. Rust, "An emerging flux model for the solar phenomenon," *Astrophysical Journal* **216**, 123–137 (1977).

- ¹¹⁸V. Archontis, F. Moreno-Insertis, K. Galsgaard, A. Hood, and E. O'Shea, "Emergence of magnetic flux from the convection zone into the corona," *Astronomy and Astrophysics* **426**, 1047–1063 (2004).
- ¹¹⁹V. Archontis, F. Moreno-Insertis, K. Galsgaard, and A. W. Hood, "The Three-dimensional Interaction between Emerging Magnetic Flux and a Large-Scale Coronal Field: Reconnection, Current Sheets, and Jets," *Astrophysical Journal* **635**, 1299–1318 (2005).
- ¹²⁰K. Galsgaard, F. Moreno-Insertis, V. Archontis, and A. Hood, "A Three-dimensional Study of Reconnection, Current Sheets, and Jets Resulting from Magnetic Flux Emergence in the Sun," *Astrophysical Journal* **618**, L153–L156 (2005), [arXiv:astro-ph/0410057 \[astro-ph\]](#).
- ¹²¹V. Archontis and A. W. Hood, "Magnetic flux emergence: a precursor of solar plasma expulsion," *Astronomy and Astrophysics* **537**, A62 (2012).
- ¹²²V. Archontis, "Magnetic flux emergence and associated dynamic phenomena in the Sun," *Philosophical Transactions of the Royal Society of London Series A* **370**, 3088–3113 (2012).
- ¹²³F. Moreno-Insertis and K. Galsgaard, "Plasma Jets and Eruptions in Solar Coronal Holes: A Three-dimensional Flux Emergence Experiment," *Astrophysical Journal* **771**, 20 (2013), [arXiv:1305.2201 \[astro-ph.SR\]](#).
- ¹²⁴N. E. Raouafi, S. Patsourakos, E. Pariat, P. R. Young, A. C. Sterling, A. Savcheva, M. Shimojo, F. Moreno-Insertis, C. R. DeVore, V. Archontis, T. Török, H. Mason, W. Curdt, K. Meyer, K. Dalmasse, and Y. Matsui, "Solar Coronal Jets: Observations, Theory, and Modeling," *Space Science Reviews* **201**, 1–53 (2016).
- ¹²⁵P. F. Wyper, C. R. DeVore, J. T. Karpen, and B. J. Lynch, "Three-Dimensional Simulations of Tearing and Intermittency in Coronal Jets," *Astrophysical Journal* **827**, 4 (2016).
- ¹²⁶P. F. Wyper, S. K. Antiochos, and C. R. DeVore, "A universal model for solar eruptions," *Nature* **544**, 452–455 (2017).
- ¹²⁷V. Archontis and A. W. Hood, "A Numerical Model of Standard to Blowout Jets," *Astrophysical Journal* **769**, L21 (2013).
- ¹²⁸M. El-Alaoui, R. J. Walker, J. M. Weygand, G. Lapenta, and M. L. Goldstein, "Magnetohydrodynamic turbulence in the earth's magnetotail from observations and global mhd simulations," *Frontiers in Astronomy and Space Sciences* **8**, 23 (2021).
- ¹²⁹L.-J. Chen, J. Ng, Y. Omelchenko, and S. Wang, "Magnetopause Reconnection and Indents Induced by Foreshock Turbulence," *Journal of Geophysics Research* **48**, e93029 (2021), [arXiv:2103.07448 \[physics.space-ph\]](#).
- ¹³⁰K. Nishida, N. Nishizuka, and K. Shibata, "The Role of a Flux Rope Ejection in a Three-dimensional Magnetohydrodynamic Simulation of a Solar Flare," *Astrophysical Journal Letters* **775**, L39 (2013), [arXiv:1308.0442 \[astro-ph.SR\]](#).
- ¹³¹S. Inoue, "Magnetohydrodynamics modeling of coronal magnetic field and solar eruptions based on the photospheric magnetic field," *Progress in Earth and Planetary Science* **3**, 19 (2016).
- ¹³²S. Inoue, D. Shiota, Y. Bamba, and S.-H. Park, "Magnetohydrodynamic Modeling of a Solar Eruption Associated with an X9.3 Flare Observed in the Active Region 12673," *Astrophysical Journal* **867**, 83 (2018).
- ¹³³X. Cheng, Y. Li, L. F. Wan, M. D. Ding, P. F. Chen, J. Zhang, and J. J. Liu, "Observations of Turbulent Magnetic Reconnection within a Solar Current Sheet," *Astrophysical Journal* **866**, 64 (2018), [arXiv:1808.06071 \[astro-ph.SR\]](#).
- ¹³⁴R. B. Decker, "Computer modeling of test particle acceleration at oblique shocks," *Space Science Reviews* **48**, 195–262 (1988).
- ¹³⁵E. Fermi, "Galactic Magnetic Fields and the Origin of Cosmic Radiation," *Astrophys. J.* **119**, 1 (1954).
- ¹³⁶L. O. Drury, "An introduction to the theory of diffusive shock acceleration of energetic particles in tenuous plasmas," *Reports on Progress in Physics* **46**, 973–1027 (1983).
- ¹³⁷R. B. Decker and L. Vlahos, "Numerical Studies of Particle Acceleration at Turbulent, Oblique Shocks with an Application to Prompt Ion Acceleration during Solar Flares," *Astrophysical Journal* **306**, 710 (1986).
- ¹³⁸A. R. Bell, "The acceleration of cosmic rays in shock fronts. I," *MNRAS* **182**, 147–156 (1978).
- ¹³⁹A. R. Bell, "The acceleration of cosmic rays in shock fronts. II," *MNRAS* **182**, 443–455 (1978).
- ¹⁴⁰D. Burgess, P. Hellinger, I. Gingell, and P. M. Trávníček, "Microstructure in two- and three-dimensional hybrid simulations of perpendicular collisionless shocks," *Journal of Plasma Physics* **82**, 905820401 (2016), [arXiv:1601.01570 \[physics.space-ph\]](#).
- ¹⁴¹N. Omid, "Formation of cavities in the foreshock," in *Turbulence and Nonlinear Processes in Astrophysical Plasmas*, American Institute of Physics Conference Series, Vol. 932, edited by D. Shaikh and G. P. Zank (2007) pp. 181–190.
- ¹⁴²I. Gingell, S. J. Schwartz, J. P. Eastwood, J. E. Stawarz, J. L. Burch, R. E. Ergun, S. A. Fuselier, D. J. Gershman, B. L. Giles, Y. V. Khotyaintsev, B. Lavraud, P. A. Lindqvist, W. R. Paterson, T. D. Phan, C. T. Russell, R. J. Strangeway, R. B. Torbert, and F. Wilder, "Statistics of Reconnecting Current Sheets in the Transition Region of Earth's Bow Shock," *Journal of Geophysical Research (Space Physics)* **125**, e27119 (2020).
- ¹⁴³Q. Lu, H. Wang, X. Wang, S. Lu, R. Wang, X. Gao, and S. Wang, "Turbulence-Driven Magnetic Reconnection in the Magnetosheath Downstream of a Quasi-Parallel Shock: A Three-Dimensional Global Hybrid Simulation," *Journal of Geophysics Research* **47**, e85661 (2020).
- ¹⁴⁴S. Lu, R. Wang, Q. Lu, V. Angelopoulos, R. Nakamura, A. V. Artemyev, P. L. Pritchett, T. Z. Liu, X. J. Zhang, W. Baumjohann, W. Gonzalez, A. C. Rager, R. B. Torbert, B. L. Giles, D. J. Gershman, C. T. Russell, R. J. Strangeway, Y. Qi, R. E. Ergun, P. A. Lindqvist, J. L. Burch, and S. Wang, "Magnetotail reconnection onset caused by electron kinetics with a strong external driver," *Nature Communications* **11**, 5049 (2020).
- ¹⁴⁵J. A. Kropotina, L. Webster, A. V. Artemyev, A. M. Bykov, D. L. Vainchtein, and I. Y. Vasko, "Solar Wind Discontinuity Transformation at the Bow Shock," *Astrophysical Journal* **913**, 142 (2021), [arXiv:2106.06414 \[physics.space-ph\]](#).
- ¹⁴⁶D. Trotta, F. Valentini, D. Burgess, and S. Servidio, "Phase space transport in the interaction between shocks and plasma turbulence," *Proceedings of the National Academy of Science* **118**, 2026764118 (2021).
- ¹⁴⁷G. K. Parks, E. Lee, Z. W. Yang, N. Lin, S. Y. Fu, and Y. Liu, "Solar Wind Interaction with Earth's Bow Shock," in *Magnetospheres in the Solar System*, Vol. 2, edited by R. Maggiolo, N. André, H. Hasegawa, and D. T. Welling (2021) p. 125.
- ¹⁴⁸I. Gingell, S. J. Schwartz, D. Burgess, A. Johlander, C. T. Russell, J. L. Burch, R. E. Ergun, S. Fuselier, D. J. Gershman, B. L. Giles, K. A. Goodrich, Y. V. Khotyaintsev, B. Lavraud, P.-A. Lindqvist, R. J. Strangeway, K. Trattner, R. B. Torbert, H. Wei, and F. Wilder, "MMS Observations and Hybrid Simulations of Surface Ripples at a Marginally Quasi-Parallel Shock," *Journal of Geophysical Research (Space Physics)* **122**, 11,003–11,017 (2017).
- ¹⁴⁹D. Burgess, E. A. Lucek, M. Scholer, S. D. Bale, M. A. Balikhin, A. Balogh, T. S. Horbury, V. V. Krasnoselskikh, H. Kucharek, B. Lembège, E. Möbius, S. J. Schwartz, M. F. Thomsen, and S. N. Walker, "Quasi-parallel Shock Structure and Processes," *Space Science Reviews* **118**, 205–222 (2005).
- ¹⁵⁰L. B. Wilson, A. Koval, D. G. Sibeck, A. Szabo, C. A. Cattell, J. C. Kasper, B. A. Maruca, M. Pulupa, C. S. Salem, and M. Wilber, "Shocklets, SLAMS, and field-aligned ion beams in the terrestrial foreshock," *Journal of Geophysical Research (Space Physics)* **118**, 957–966 (2013), [arXiv:1207.5561 \[physics.space-ph\]](#).
- ¹⁵¹M. Palmroth, H. Hietala, F. Plaschke, M. Archer, T. Karlsson, X. Blanco-Cano, D. Sibeck, P. Kajdič, U. Ganse, Y. Pfau-Kempf, M. Battarbee, and L. Turc, "Magnetosheath jet properties and evolution as determined by a global hybrid-Vlasov simulation," *Annales Geophysicae* **36**, 1171–1182 (2018).
- ¹⁵²Y. Matsumoto, T. Amano, T. N. Kato, and M. Hoshino,

- “Stochastic electron acceleration during spontaneous turbulent reconnection in a strong shock wave,” *Science* **347**, 974–978 (2015).
- ¹⁵³D. Caprioli and C. Haggerty, “The Issue with Diffusive Shock Acceleration,” in *36th International Cosmic Ray Conference (ICRC2019)*, International Cosmic Ray Conference, Vol. 36 (2019) p. 209, [arXiv:1909.06288 \[astro-ph.HE\]](#).
- ¹⁵⁴D. Caprioli, C. C. Haggerty, and P. Blasi, “Kinetic Simulations of Cosmic-Ray-modified Shocks. II. Particle Spectra,” *Astrophysical Journal* **905**, 2 (2020), [arXiv:2009.00007 \[astro-ph.HE\]](#).
- ¹⁵⁵D. Caprioli and A. Spitkovsky, “Simulations of Ion Acceleration at Non-relativistic Shocks. I. Acceleration Efficiency,” *Astrophys. J.* **783**, 91 (2014), [arXiv:1310.2943 \[astro-ph.HE\]](#).
- ¹⁵⁶D. Trotta, F. Pecora, A. Settino, D. Perrone, H. Hietala, T. Horbury, W. Matthaeus, D. Burgess, S. Servidio, and F. Valentini, “On the Transmission of Turbulent Structures across the Earth’s Bow Shock,” *Astrophys. J.* **933**, 167 (2022), [arXiv:2202.14029 \[physics.space-ph\]](#).
- ¹⁵⁷Z. Guo, Y. Lin, and X. Wang, “Global Hybrid Simulations of Interaction Between Interplanetary Rotational Discontinuity and Bow Shock/Magnetosphere: Can Ion Scale Magnetic Reconnection be Driven by Rotational Discontinuity Downstream of Quasi Parallel Shock?” *Journal of Geophysical Research (Space Physics)* **126**, e28853 (2021).
- ¹⁵⁸T. Gold, “Magnetic Energy Shedding in the Solar Atmosphere,” in *NASA Special Publication*, Vol. 50 (1964) p. 389.
- ¹⁵⁹E. N. Parker, “Topological Dissipation and the Small-Scale Fields in Turbulent Gases,” *Astrophysical Journal* **174**, 499 (1972).
- ¹⁶⁰W. M. Glencross, “Heating of coronal material at X-ray bright points,” *Astrophysical Journal Letters* **199**, L53–L56 (1975).
- ¹⁶¹R. H. Levine, “A New Theory of Coronal Heating,” *Astrophysical Journal* **190**, 457–466 (1974).
- ¹⁶²P. A. Sturrock and Y. Uchida, “Coronal heating by stochastic magnetic pumping,” *Astrophysical Journal* **246**, 331–336 (1981).
- ¹⁶³C. Chiuderi, “Keys to understanding the corona,” in *ESA Special Publication*, ESA Special Publication, Vol. 1157, edited by P. Maltby and B. Battrock (1993) pp. 25–32.
- ¹⁶⁴N. B. Crosby, M. J. Aschwanden, and B. R. Dennis, “Frequency distributions and correlations of solar X-ray flare parameters,” *Solar Physics* **143**, 275–299 (1993).
- ¹⁶⁵N. B. Crosby, “Frequency distributions: from the sun to the earth,” *Nonlinear Processes in Geophysics* **18**, 791–805 (2011).
- ¹⁶⁶M. J. Aschwanden, N. B. Crosby, M. Dimitropoulou, M. K. Georgoulis, S. Hergarten, J. McAteer, A. V. Milovanov, S. Mineshige, L. Morales, N. Nishizuka, G. Pruessner, R. Sanchez, A. S. Sharma, A. Strugarek, and V. Uritsky, “25 Years of Self-Organized Criticality: Solar and Astrophysics,” *Space Science Review* **198**, 47–166 (2016), [arXiv:1403.6528 \[astro-ph.IM\]](#).
- ¹⁶⁷Z. Mikic, D. D. Schnack, and G. van Hoven, “Creation of current filaments in the solar corona,” *Astroph. J.* **338**, 1148–1157 (1989).
- ¹⁶⁸G. Einaudi, M. Velli, H. Politano, and A. Pouquet, “Energy Release in a Turbulent Corona,” *Astrophys. J. Letters* **457**, L113 (1996).
- ¹⁶⁹M. K. Georgoulis, M. Velli, and G. Einaudi, “Statistical Properties of Magnetic Activity in the Solar Corona,” *Astrophys. J.* **497**, 957–966 (1998).
- ¹⁷⁰A. F. Rappazzo, M. Velli, and G. Einaudi, “Shear Photospheric Forcing and the Origin of Turbulence in Coronal Loops,” *Astroph. J.* **722**, 65–78 (2010), [arXiv:1003.3872 \[astro-ph.SR\]](#).
- ¹⁷¹V. Hansteen, B. De Pontieu, M. Carlsson, J. Lemen, A. Title, P. Boerner, N. Hurlburt, T. D. Tarbell, J. P. Wuelser, T. M. D. Pereira, E. E. De Luca, L. Golub, S. McKillop, K. Reeves, S. Saar, P. Testa, H. Tian, C. Kankelborg, S. Jaeggli, L. Kleint, and J. Martínez-Sykora, “The unresolved fine structure resolved: IRIS observations of the solar transition region,” *Science* **346**, 1255757 (2014), [arXiv:1412.3611 \[astro-ph.SR\]](#).
- ¹⁷²R. B. Dahlburg, G. Einaudi, B. D. Taylor, I. Ugarte-Urra, H. P. Warren, A. F. Rappazzo, and M. Velli, “Observational Signatures of Coronal Loop Heating and Cooling Driven by Footpoint Shuffling,” *Astroph. J.* **817**, 47 (2016), [arXiv:1512.03079 \[astro-ph.SR\]](#).
- ¹⁷³C. Kanella and B. V. Gudiksen, “Identification of coronal heating events in 3D simulations,” *Astronomy and Astrophysics* **603**, A83 (2017), [arXiv:1703.02808 \[astro-ph.SR\]](#).
- ¹⁷⁴C. Kanella and B. V. Gudiksen, “Investigating 4D coronal heating events in magnetohydrodynamic simulations,” *Astronomy and Astrophysics* **617**, A50 (2018), [arXiv:1806.04495 \[astro-ph.SR\]](#).
- ¹⁷⁵V. Hansteen, A. Ortiz, V. Archontis, M. Carlsson, T. M. D. Pereira, and J. P. Bjørgen, “Ellerman bombs and UV bursts: transient events in chromospheric current sheets,” *Astronomy and Astrophysics* **626**, A33 (2019), [arXiv:1904.11524 \[astro-ph.SR\]](#).
- ¹⁷⁶R. Turkmani, L. Vlahos, K. Galsgaard, P. Cargill, and H. Isliker, “Particle acceleration in stressed coronal magnetic fields,” *The Astrophysical Journal Letters* **620**, L59 (2005).
- ¹⁷⁷R. Turkmani, P. Cargill, K. Galsgaard, L. Vlahos, and H. Isliker, “Particle acceleration in stochastic current sheets in stressed coronal active regions,” *Astronomy & Astrophysics* **449**, 749–757 (2006).
- ¹⁷⁸A. F. Rappazzo, M. Velli, and G. Einaudi, “Field Lines Twisting in a Noisy Corona: Implications for Energy Storage and Release, and Initiation of Solar Eruptions,” *Astroph. J.* **771**, 76 (2013), [arXiv:1301.7678 \[astro-ph.SR\]](#).
- ¹⁷⁹A. F. Rappazzo and E. N. Parker, “Current Sheets Formation in Tangled Coronal Magnetic Fields,” *Astroph. J. Letters* **773**, L2 (2013), [arXiv:1306.6634 \[astro-ph.SR\]](#).
- ¹⁸⁰A. F. Rappazzo, W. H. Matthaeus, D. Ruffolo, M. Velli, and S. Servidio, “Coronal Heating Topology: The Interplay of Current Sheets and Magnetic Field Lines,” *Astroph. J.* **844**, 87 (2017), [arXiv:1706.08983 \[astro-ph.SR\]](#).
- ¹⁸¹J. Threlfall, J. Reid, and A. W. Hood, “Can Multi-threaded Flux Tubes in Coronal Arcades Support a Magnetohydrodynamic Avalanche?” *Solar Physics* **296**, 120 (2021), [arXiv:2107.08758 \[astro-ph.SR\]](#).
- ¹⁸²V. Archontis and V. Hansteen, “Clusters of Small Eruptive Flares Produced by Magnetic Reconnection in the Sun,” *Astroph. J.* **788**, L2 (2014), [arXiv:1405.6420 \[astro-ph.SR\]](#).
- ¹⁸³C. Kanella and B. V. Gudiksen, “Emission of Joule heating events in simulations of the solar corona,” *Astronomy and Astrophysics* **621**, A95 (2019).
- ¹⁸⁴M. C. M. Cheung, M. Rempel, G. Chintzoglou, F. Chen, P. Testa, J. Martínez-Sykora, A. Sainz Dalda, M. L. DeRosa, A. Malanushenko, V. Hansteen, B. De Pontieu, M. Carlsson, B. Gudiksen, and S. W. McIntosh, “A comprehensive three-dimensional radiative magnetohydrodynamic simulation of a solar flare,” *Nature Astronomy* **3**, 160–166 (2019).
- ¹⁸⁵S. Inoue, K. Hayashi, T. Miyoshi, J. Jing, and H. Wang, “A Comparative Study of Solar Active Region 12371 with Data-constrained and Data-driven Magnetohydrodynamic Simulations,” *Astrophysical Journal Letters* **944**, L44 (2023), [arXiv:2301.12336 \[astro-ph.SR\]](#).
- ¹⁸⁶W. He, C. Jiang, P. Zou, A. Duan, X. Feng, P. Zuo, and Y. Wang, “Data-driven MHD Simulation of the Formation and Initiation of a Large-scale Preflare Magnetic Flux Rope in AR 12371,” *Astrophysical Journal* **892**, 9 (2020), [arXiv:2002.04837 \[astro-ph.SR\]](#).
- ¹⁸⁷C. Jiang, X. Feng, R. Liu, X. Yan, Q. Hu, R. L. Moore, A. Duan, J. Cui, P. Zuo, Y. Wang, and F. Wei, “A fundamental mechanism of solar eruption initiation,” *Nature Astronomy* **5**, 1126–1138 (2021), [arXiv:2107.08204 \[astro-ph.SR\]](#).
- ¹⁸⁸M. Gordovskyy and P. K. Browning, “Particle Acceleration by Magnetic Reconnection in a Twisted Coronal Loop,” *Astrophys. J.* **729**, 101 (2011).
- ¹⁸⁹L. Vlahos and H. Isliker, “Complexity methods applied to turbulence in plasma astrophysics,” *European Physical Journal Special Topics* **225** (2016), 10.1140/epjst/e2016-02650-7,

- [arXiv:1603.00394 \[astro-ph.SR\]](#).
- ¹⁹⁰B. Chopard and M. Droz, "*Cellular Automata Modeling of Physical Systems*" (Cambridge University Press, Cambridge, UK, 2005).
 - ¹⁹¹E. T. Lu and R. J. Hamilton, "Avalanches and the distribution of solar flares," *Astroph. J. Letters* **380**, L89–L92 (1991).
 - ¹⁹²P. Bak, C. Tang, and K. Wiesenfeld, "Self-organized criticality - An explanation of $1/f$ noise," *Physical Review Letters* **59**, 381–384 (1987).
 - ¹⁹³P. Charbonneau, S. W. McIntosh, H.-L. Liu, and T. J. Bogdan, "Avalanche models for solar flares (Invited Review)," *Solar Physics* **203**, 321–353 (2001).
 - ¹⁹⁴M. J. Aschwanden, *Self-Organized Criticality in Astrophysics* (Springer-Praxis, Berlin, 2011).
 - ¹⁹⁵H. Isliker, A. Anastasiadis, and L. Vlahos, "MHD consistent cellular automata (CA) models. I. Basic features," *Astronomy and Astrophysics* **363**, 1134–1144 (2000), [astro-ph/0106111](#).
 - ¹⁹⁶H. Isliker, A. Anastasiadis, and L. Vlahos, "MHD consistent cellular automata (CA) models. II. Applications to solar flares," *Astronomy and Astrophysics* **377**, 1068–1080 (2001), [astro-ph/0108365](#).
 - ¹⁹⁷L. Vlahos, M. Georgoulis, R. Kluiving, and P. Paschos, "The statistical flare," *Astronomy and Astrophysics* **299**, 897 (1995).
 - ¹⁹⁸M. K. Georgoulis and L. Vlahos, "Coronal Heating by Nanoflares and the Variability of the Occurrence Frequency in Solar Flares," *Astrophys. J.* **469**, L135 (1996).
 - ¹⁹⁹M. K. Georgoulis and L. Vlahos, "Variability of the occurrence frequency of solar flares and the statistical flare," *Astronomy and Astrophysics* **336**, 721–734 (1998).
 - ²⁰⁰E. T. Lu, R. J. Hamilton, J. M. McTiernan, and K. R. Bromund, "Solar flares and avalanches in driven dissipative systems," *Astrophys. J.* **412**, 841–852 (1993).
 - ²⁰¹H. Isliker, A. Anastasiadis, D. Vassiliadis, and L. Vlahos, "Solar flare cellular automata interpreted as discretized MHD equations," *Astronomy and Astrophysics* **335**, 1085–1092 (1998).
 - ²⁰²W. H. Press, S. A. Teukolsky, W. T. Vetterling, and B. P. Flannery, *Cambridge: University Press, —c1992, 2nd ed.* (1992).
 - ²⁰³T. Fragos, E. Rantsiou, and L. Vlahos, "On the distribution of magnetic energy storage in solar active regions," *Astronomy and Astrophysics* **420**, 719–728 (2004).
 - ²⁰⁴K. Moraitis, A. Toutountzi, H. Isliker, M. Georgoulis, L. Vlahos, and G. Chintzoglou, "An observationally-driven kinetic approach to coronal heating," *Astr. Astrophys.* **596**, A56 (2016), [arXiv:1603.07129 \[astro-ph.SR\]](#).
 - ²⁰⁵M. Dimitropoulou, H. Isliker, L. Vlahos, and M. K. Georgoulis, "Simulating flaring events in complex active regions driven by observed magnetograms," *Astronomy and Astrophysics* **529**, A101 (2011), [arXiv:1102.2352 \[astro-ph.SR\]](#).
 - ²⁰⁶M. Dimitropoulou, H. Isliker, L. Vlahos, and M. K. Georgoulis, "Dynamic data-driven integrated flare model based on self-organized criticality," *Astronomy and Astrophysics* **553**, A65 (2013).
 - ²⁰⁷L. Vlahos, "Theory of fragmented energy release in the Sun," *Space Science Reviews* **68**, 39–50 (1994).
 - ²⁰⁸A. Anastasiadis and L. Vlahos, "Particle acceleration in an evolving active region by an ensemble of shock waves," *Astrophys. J.* **428**, 819–826 (1994).
 - ²⁰⁹V. M. Uritsky, M. Paczuski, J. M. Davila, and S. I. Jones, "Co-existence of Self-Organized Criticality and Intermittent Turbulence in the Solar Corona," *Physical Review Letters* **99**, 025001 (2007), [astro-ph/0610130](#).
 - ²¹⁰V. M. Uritsky and J. M. Davila, "Multiscale Dynamics of Solar Magnetic Structures," *Astrophys. J.* **748**, 60 (2012), [arXiv:1111.5053 \[astro-ph.SR\]](#).
 - ²¹¹R. B. Dahlburg, J. A. Klimchuk, and S. K. Antiochos, "An Explanation for the "Switch-On" Nature of Magnetic Energy Release and Its Application to Coronal Heating," *Astrophys. J.* **622**, 1191–1201 (2005).